

## CALCAREOUS NANNOFOSSIL TAXONOMY AND BIOSTRATIGRAPHY OF THE TOARCIAN-LOWER BAJOCIAN COLLE DI SOGNO SECTION (LOMBARDY BASIN, SOUTHERN ALPS, ITALY)

STEFANO VISENTIN<sup>1</sup>, GIULIA FAUCHER<sup>1</sup> & ELISABETTA ERBA<sup>1\*</sup>

<sup>1</sup>Dipartimento di Scienze della Terra “Ardito Desio”, Università degli Studi di Milano, Via Mangiagalli 34, 20133 Milano, Italy

\*Corresponding author. E-mail: [elisabetta.erba@unimi.it](mailto:elisabetta.erba@unimi.it)

Associate Editor: Silvia Gardin.

To cite this article: Visentin S., Faucher G. & Erba E. (2023) - Calcareous nannofossil taxonomy and biostratigraphy of the Toarcian-lower Bajocian Colle di Sogno section (Lombardy Basin, Southern Alps, Italy). *Riv. It. Paleontol. Strat.*, 129(1): 207-228.

---

**Keywords:** Calcareous nannofossils; Toarcian – lower Bajocian; biostratigraphy; *Watznaueria* taxonomy and evolution.

**Abstract:** Calcareous nannofossil biostratigraphy was conducted in the Toarcian-lower Bajocian interval at Colle di Sogno (Lombardy Basin, Southern Alps, Northern Italy) where the type-section of the Sogno Formation consisting of pelagic marly limestone, marlstone and marly claystone was established. Semiquantitative analyses of calcareous nannofossil assemblages allowed to achieve a high-resolution biostratigraphy based on several biohorizons, including zonal/subzonal markers and additional events. The NJT5 to NJT9 Zones of the standard nannofossil zonation established for the Mediterranean Province were identified. The biostratigraphy obtained at Colle di Sogno was compared to published nannofossil events calibrated with ammonite zones in sections from SE Spain, S France, Portugal and N Algeria. This assessment evidenced some discrepancies in the succession of events of the standard zonation and, furthermore, resulted in the revision of the age of a few datums. Moreover, some new/additional nannofossil biohorizons are proposed as subzonal markers.

A morphometric analysis of the genus *Watznaueria* was conducted to identify diagnostic features for unambiguous species identification. The species *W. colacicchi* and *W. contracta* are distinguished on the basis of the coccolith width/central area width ratio, whereas *W. britannica britannica* is discriminated by the size - as in the original definition of the species - relative to the new subspecies *W. britannica minor*. The new species *W. gaetanii* differs from all other *Watznaueria* taxa by the bridge ultrastructure. In the Toarcian-Aalenian interval a progressive increase in size of *Watznaueria* specimens is paralleled by the progressive closure of the central area and the modification of the central area structure passing from a cross (*W. colacicchi* and *W. contracta*) to a double-button bridge (*W. gaetanii*) to a single-button bridge (*W. britannica*). These intrageneric evolutionary innovations accelerated in the Aalenian under stable paleoceanographic conditions and an oligotrophic regime.

## INTRODUCTION

Pelagic sedimentary successions consist of biogenic particles with minor to absent contribution by siliciclastic input. Since Jurassic times, pelagic micrites have been accumulated on the sea-floor as the result of calcareous nannoplankton production and their sinking through the water column after death. During the Early-Middle Jurassic nannofloras experienced major speciation episodes and some of the most common Jurassic and Cretaceous genera (*Biscutum*, *Lotbaringius*, *Discorhabdus* and *Watznaueria*) appeared and evolved (Bown 1987; Mattioli & Erba 1999; Bown et al. 2004; Erba 2006; Suchéras-Marx et al. 2015). The abundance, taxonomic diversity, rapid evolution and wide distribution of Jurassic calcareous nannofossils in marine environments were recognized as instrumental for biostratigraphy. Indeed, the considerable number of calcareous nannofossil biohorizons characterizing the late Pliensbachian-early Bajocian time interval resulted in high-resolution biozonations. However, Jurassic nannoplankton paleoprovincialism has determined the establishment of different biostratigraphic schemes applicable in the Boreal Realm (Bown & Cooper 1998), the Tethyan area (Mattioli & Erba 1999) and Portugal (Ferreira et al. 2019).

Biostratigraphic investigations of hemipelagic-pelagic sections in the western Tethys Ocean have shown that the biozonation of Mattioli & Erba (1999), although still fully valid, can be improved both in terms of stratigraphic resolution and revision of event ages (e.g. Casellato & Erba 2015; Ferreira et al. 2019; Visentin & Erba 2021). Furthermore, a reexamination of the events used for the standard Tethyan biozonation (Mattioli & Erba 1999) is required following the revised taxonomy of some genera and species (Giraud et al. 2006; Giraud 2009; Visentin et al. 2021a).

We investigated calcareous nannofossils in the Toarcian-lower Bajocian interval of the Colle di Sogno section located in the Lombardy Basin within the Southern Alps (Northern Italy) (Fig.1). This outcrop is the type-section of the Sogno Formation (Gaetani & Poliani 1978) consisting of pelagic marly limestone, marlstone and marly claystone. The Colle di Sogno succession was previously characterized with calcareous nannofossil biostratigraphy gained for the uppermost Pliensbachian-lower Toarcian portion (Casellato & Erba 2015). The same interval

was also recovered with the Sogno Core (Erba et al. 2019a; Erba et al. 2022) that was investigated for high-resolution nannofossil biostratigraphy (Visentin & Erba 2021). In this study, we extend the nannofloral characterization up to the lower Bajocian portion of the Colle di Sogno section to gain a detailed nannofossil biostratigraphy of the Toarcian-lower Bajocian interval. The expected high-resolution nannofossil biostratigraphy will be the basis for a reevaluation of the Mattioli & Erba (1999) standard Tethyan zonation.

Giraud et al. (2006) characterized the morphological variability of *Watznaueria britannica* that is a marker species in the standard biozonations. Some of the morphogroups identified in the Oxfordian were applied in biostratigraphic studies of Toarcian-Aalenian sections (Ferreira et al. 2019) resulting in a revised age of the appearance level of *W. britannica* and, accordingly, of the nominal zone. However, some diagnostic differences of the six morphotypes, namely size ranges, are elusive and difficult to objectively identify. The same problem also arose for *W. colacicchii* and *W. contracta* (see comments of the nannotax website <https://www.mikrotax.org/system/index.php?id=10595>), which are also biostratigraphic markers of the standard zonations. For these reasons, we conducted a morphometric analysis of the genus *Watznaueria* aimed at the identification of diagnostic features for clarification of species differences and determination. This is particularly crucial for the investigated interval because it was the time of emergence and early diversification of the genus *Watznaueria*.

## GEOLOGICAL SETTING AND LITHOSTRATIGRAPHY

The Lombardy Basin was part of the undeformed portion of the margin of the Adria microplate in the western Tethys Ocean (Gaetani 2010) (Fig. 1). During the latest Triassic to earliest Jurassic time interval rifting pulses disrupted an extensive shallow-water carbonate platform producing a bathymetry shaped by synsedimentary horst and graben structures in a pelagic setting (Bernoulli & Jenkyns 1974, 2009; Winterer & Bosellini 1981; Bosence et al. 2009; Santantonio & Carminati 2011; Jenkyns 2020). As a consequence, during the Jurassic different sedimentary regimes characterized the

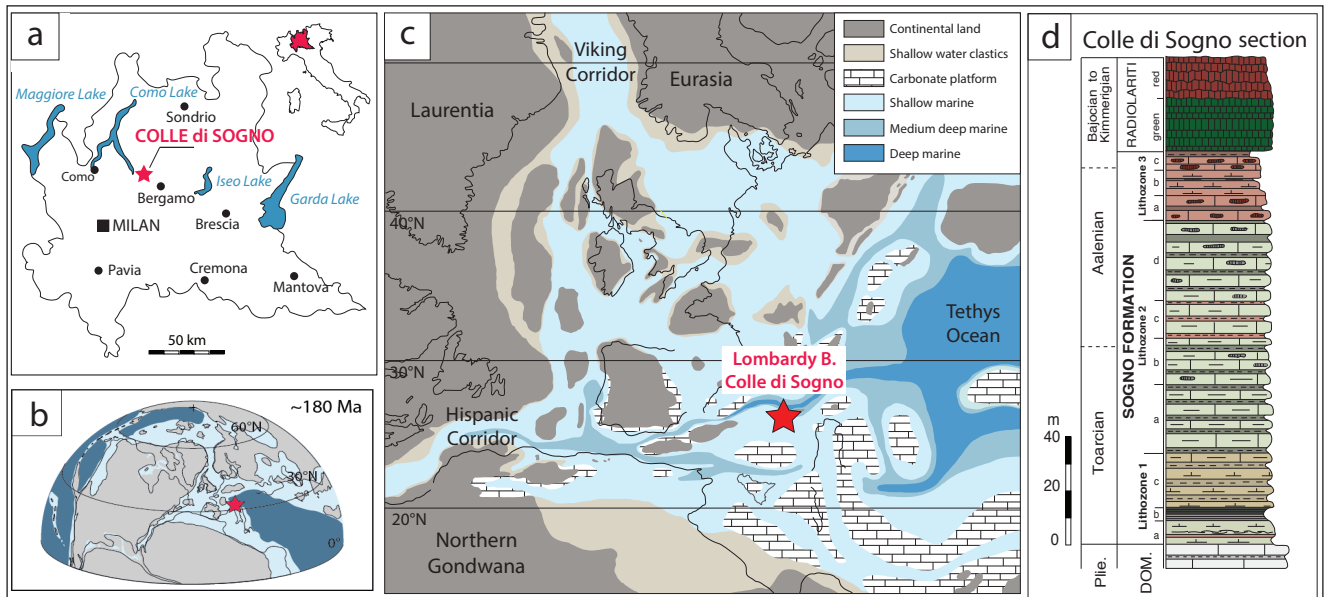


Fig.1 - A) Present-day location of the Colle di Sogno section. B, C) Paleogeographic location of the studied section during the Toarcian (~180 Ma) (modified after Scotese 2011). D) Simplified lithostratigraphy of the uppermost Pliensbachian to Kimmeridgian Colle di Sogno section.

deeper zones with thick, complete and continuous successions, whereas structural highs with condensed and incomplete sequences (Gaetani 1975, 2010). Since the Early Jurassic the Lombardy Basin became a pelagic area between the Lugano High to the west and the Trento Plateau to the east, further subdivided into intrabasinal troughs and palaeohighs that are, from west to east: Monte Nudo Trough, Lugano High, Generoso Trough, Corni di Canzo High, Albenza Plateau, Monte Cavallo High, Sebino Trough, Botticino High.

The Colle di Sogno section is exposed along the road SP 179 on the northern slope of Mt. Brughetto (45° 47' 29" N, 9° 28' 44" E) (Gaetani & Poliani 1978; Jenkyns & Clayton 1986; Gaetani & Erba 1990; Hinnov et al. 2000; Muttoni et al. 2005; Channell et al. 2010; Casellato & Erba 2015) (Fig. 1). The Sinemurian-lower Bajocian interval consists of pelagic limestone, marly limestone, marlstone and marly claystone, followed by stratified chert and cherty limestone of Bajoacian-Kimmeridgian age (Muttoni et al. 2005). The sequence of the Colle di Sogno section deposited on a pelagic plateau (Albenza Plateau) (Gaetani & Erba 1990; Pasquini & Vercesi 2002; Gaetani 2010) at a paleowater depth of about 1500 metres during the Early-Middle Jurassic (Erba et al. 2022).

For the present study, calcareous nannofossils were investigated with respect to their abundance

and diversity patterns, revisiting the uppermost Pliensbachian-lowermost Toarcian interval documented by Casellato & Erba (2015) and extending the analyses upwards to the lower Bajocian (basal part of the Radiolarite Formation). The Sogno Formation, sandwiched by the underlying Domare Limestone and the overlying Radiolarite formations, was lithostratigraphically subdivided into three lithozones. These can be further split into sub-units (a-c), from bottom to top:

**Lithozone 1:** this lithozone has a thickness of 31.20 m. The lowermost 27 cm of this unit consist of greenish marly claystone followed by 8 metres of greenish and reddish marlstone and limy marlstone in 25 to 5 cm-thick beds (Lithozone 1a). A slumped interval was detected between 2.90 m and 4.75 m. A carbonate-poor, black shale interval named Fish Level (Gaetani & Poliani 1978; Casellato & Erba 2015; Erba et al. 2022) consists of dark greenish-grey marly claystone in the lower portion (8.27-10.73 m) and dark brown marly claystone to fissile black shale in the upper part (10.73-12.98 m) (Lithozone 1b = Fish Level = 4.71 m). Above the Fish Level a 18.22 m interval comprises light brownish grey marlstone and limy marlstone organized in 20 to 40 cm-thick strata (Lithozone 1c).

**Lithozone 2:** this lithozone has a thickness of 31.20 m. The lowermost part consists of regular alternations of grey marly limestone in 20 to 60

cm-thick beds and light grey clayey marlstone, often laminated, in 20-30 cm thick beds (Lithozone 2a = 29.2 m). It is followed by a 8.6 m interval of grey marly limestone (30-40 cm beds) characterized by frequent chert lenses alternated with 10-20 cm thick grey marlstone (Lithozone 2b). The overlying interval comprises 15 metres of light grey to reddish limy marlstone and intercalated dark red clayey marlstone. Chert is absent in the Lithozone 2c. The upper part of the Lithozone 2 is characterized by light grey limy marlstone in 20-40 cm thick beds regularly intercalated with marly claystone in 5-10 cm thick beds. Chert nodules (5-10 cm long) and elongated lenses (2-4 cm thick) are frequent in the limy layers (Lithozone 2d = 27.5 m).

**Lithozone 3:** this lithozone has a thickness of 24.10 m. The lower 8.5 meters (Lithozone 3a) comprise reddish grey marly limestone in 10-30 cm thick beds alternated with reddish marlstones to marly claystone in 5-8 cm thick layers. Dark red chert nodules and lenses are common in the limy beds. The overlying Lithozone 3b consists of red marly limestone and marlstone in 10-30 cm thick beds alternated with dark red marly claystone (Lithozone 3b = 8.8 m). Lithozone 3c comprises 6.3 metres of reddish marly limestone in 10-25 cm thick beds alternated with dark red marlstones to marly claystone in 3-10 cm thick layers. Dark red chert nodules and lenses are common in the limy beds. The uppermost part of Lithozone 3c consists of 50 cm of red to dark red clayey marlstone and siliceous claystone with Fe-Mn dendrites and coatings (Lithozone 3c = 6.8 m).

## MATERIALS AND METHODS

A total of 179 samples were investigated for nannofossil biostratigraphy, with an average sampling rate of ca. 1 sample/65 cm through the studied interval. Samples were prepared from marly limestones, limy marlstones, and clayey marlstones of the Sogno Fm. (Lithozones 1, 2 and 3) and from marly claystone in the lowermost Radiolarite Fm. Standard smear slides were prepared following the method of Monechi & Thierstein (1985). For each sample, a total of 12 longitudinal traverses (corresponding to 1800 fields of views) were investigated using a light polarizing microscope Leitz Laborlux 12 POL S, at 1250X magnification. The preserva-

tion of calcareous nannofossils was evaluated using the visual criteria of Roth & Thierstein (1972) and Roth (1983) for assessment of etching (E) and overgrowth (O), with E1/O1 standing for minor, E2/O2 for moderate and E3/O3 for major etching/overgrowth. Both the total nannofloral abundance and the abundance of individual taxa were estimated. Calcareous nannofossil taxa recognized are listed in Appendix 1 and illustrated in Plates 1 and 2. The semiquantitative range chart with explanation of total and individual nannofossil abundances is reported in Appendix 2.

## RESULTS

### Calcareous nannofossil abundance and preservation

Calcareous nannofossil preservation is generally moderate, varying from poor to moderate/good through the studied section. The degree of etching/overgrowth fluctuates from E1/O1 to E3/O3, and a general higher level of overgrowth was observed compared to dissolution.

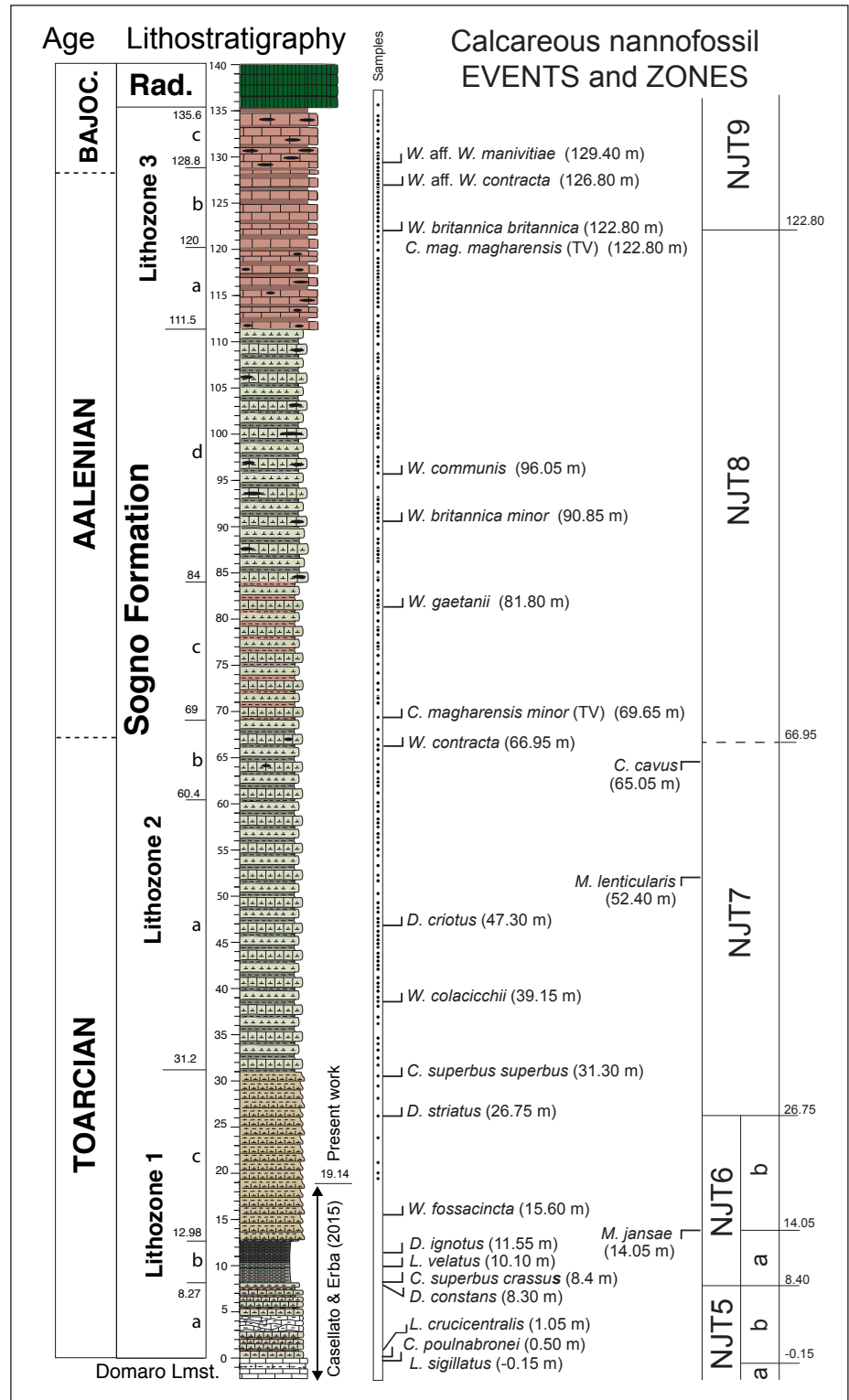
Nannofossil total abundance fluctuates from rare to frequent/common across the Sogno Fm. Very few samples in the topmost part of the Sogno Fm. (top of Lithozone 3) and lowermost Radiolarite Fm. contain extremely rare specimens or are (virtually) barren of nannofossils (Appendix 2).

### Taxonomic notes

The revision of the samples previously investigated by Casellato & Erba (2015) from the uppermost Pliensbachian-lower Toarcian interval allowed the full application of the taxonomic subdivision of the genus *Carinolithus* (Visentin et al. 2021a). All subspecies were identified resulting in an updated biostratigraphy also based on *Carinolithus* subspecies (Fig. 2).

In the middle Toarcian – lowermost Bajocian interval the *Watznaueria* species *W. colacicchii*, *W. contracta* and *W. britannica* have their first occurrence. In the studied section, along with specimens unequivocally attributable to the species above, several specimens show some characters not fully corresponding to the diagnostic features, as described in the species definitions. For this reason, a morphometric study was conducted for identifying quantitative criteria to be used for the objective identification of the

Fig. 2 – Lithostratigraphy and calcareous nannofossil biostratigraphy of the Colle di Sogno section.



*Watznaueria* species. This morphometric study was conducted on photographs taken with a Q imaging Micropublisher 5.0 RTV digital camera mounted on a Leitz Laborlux optical polarizing microscope, at 1250X magnification. Images were analysed using a PC with Q-capture Pro suite software adapted for nannofossil analyses. Measurements were taken using ImageJ software, with an error of  $\pm 0.08 \mu\text{m}$ .

### Morphometry of the *W. colacicchii* – *W. contracta* group

Morphometric analyses were performed on all specimens encountered in 4 traverses (corresponding to 600 fields of view) from 118 samples. A total of 172 specimens were found and photographed. The following parameters were measured: the coccolith length (L) and width (W) of the distal

shield and the length (l) and width (w) of the central area. Moreover, the ellipticity of the coccolith ( $L/W$ ) and the  $W/w$  ratio were calculated.

Statistical parameters (average size, median, and mode), were computed for all measured parameters. The coefficient determinations were also calculated among different parameters. The frequency distribution of  $W/w$  of *W. contracta* and *W. colacicchii* was calculated with the histogram function in R, considering each measured specimen. Each class interval includes all values that fall within the range between the minimum and maximum and is graphically represented by a bar in a histogram. The bin size is  $0.1 \mu\text{m}$  and the considered interval goes from 2 to  $6 \mu\text{m}$ . To evaluate the evolution of sizes through time, the variability of sizes has been also represented in stratigraphic order (size versus depth) considering all measured specimens and/or the average size of every sample.

The species *W. contracta* was originally assigned to the genus *Lotharingius* as *Lotharingius contractus* by Bown & Cooper (1989) who gave a range of  $L = 5.7\text{--}7.5 \mu\text{m}$  and  $W = 4.8\text{--}6.9 \mu\text{m}$ . The holotype has  $L = 7.2 \mu\text{m}$  and  $W = 6.0 \mu\text{m}$ ,  $l = 2.2 \mu\text{m}$ ,  $w = 1.5 \mu\text{m}$ . Cobianchi et al. (1992) moved the taxon to the genus *Watznaueria* and described a coccolith L range of  $5.7\text{--}7.0 \mu\text{m}$  that was later reported also by Mattioli & Erba (1999), Tiraboschi & Erba (2010), Ferreira et al. (2019), and Fantasia et al. (2021). These dimensions are, thus, different from the original description and smaller than the holotype.

The species *W. colacicchii* was established by Mattioli (1996) who described a size variability of  $L = 5.2\text{--}7.0 \mu\text{m}$  and  $W = 4.5\text{--}6.0 \mu\text{m}$ ; the holotype has  $L = 6.0 \mu\text{m}$  and  $W = 5.0 \mu\text{m}$ ,  $l = 2.2 \mu\text{m}$ ,  $w = 1.5 \mu\text{m}$ . Mattioli & Erba (1999) reported slightly smaller ranges for  $L = 5.2\text{--}6.0 \mu\text{m}$  and  $W = 4.5\text{--}5.5 \mu\text{m}$ . Mattioli (1996) compared *W. colacicchii* to *W. contracta* and highlighted as diagnostic differentiating characters a more open central area and an overall smaller size of *W. colacicchii* specimens.

The taxonomy of the Lower Jurassic *Watznaueria* species was discussed during the Jurassic nannofossil workshop held in Lyon in 2016 with the conclusion that *W. colacicchii* and *W. contracta* are not significantly different (see Nannotax website [https://www.mikrotax.org/Nannotax3/index.php?taxon=Watznaueria%20contracta&module=ntax\\_mesozoic](https://www.mikrotax.org/Nannotax3/index.php?taxon=Watznaueria%20contracta&module=ntax_mesozoic)).

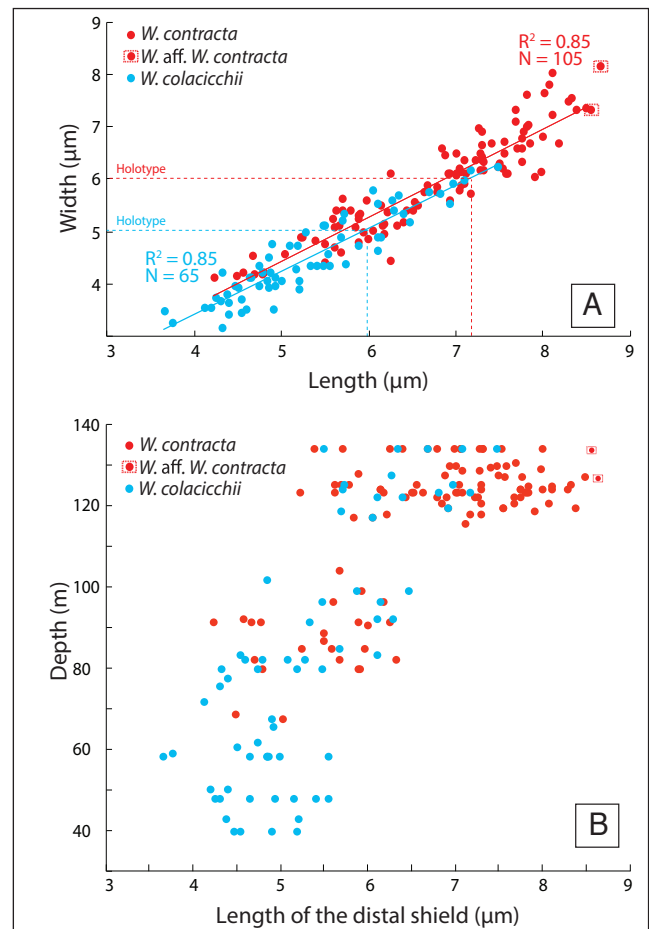


Fig. 3 – A) Scatter plots of coccolith length versus width measured in *W. colacicchii* and *W. contracta* specimens with the coefficient determinations ( $r^2$ ). The number of measurements is also given (N). The specimens that belong to *W. aff. W. contracta* are highlighted. The holotype sizes of *W. colacicchii* and *W. contracta* are also reported. B) Length of the distal shield of *W. colacicchii* and *W. contracta* versus depth of the Colle di Sogno section; the specimens that belong to *W. aff. W. contracta* are highlighted.

However, also in recent papers the two species are distinguished (Aguado et al. 2008; Sandoval et al. 2008, 2012; Ferreira et al. 2019; Fantasia et al. 2022) implying the presence of diagnostic differences. With the central area structure of *W. colacicchii* and *W. contracta* the same (a cross aligned along the ellipse axes) and the size (L and W) ranges overlapping, the species attribution is not obvious.

In the Colle di Sogno section, some specimens are not unambiguously attributable to *W. colacicchii* or *W. contracta*. Therefore, during the initial qualitative (biostratigraphic) analysis we separated the two taxa and then proceeded with quantitative measurements as suggested by Mattioli (1996) of the coccolith size (L and W) and the dimensions of the central area (l and w).

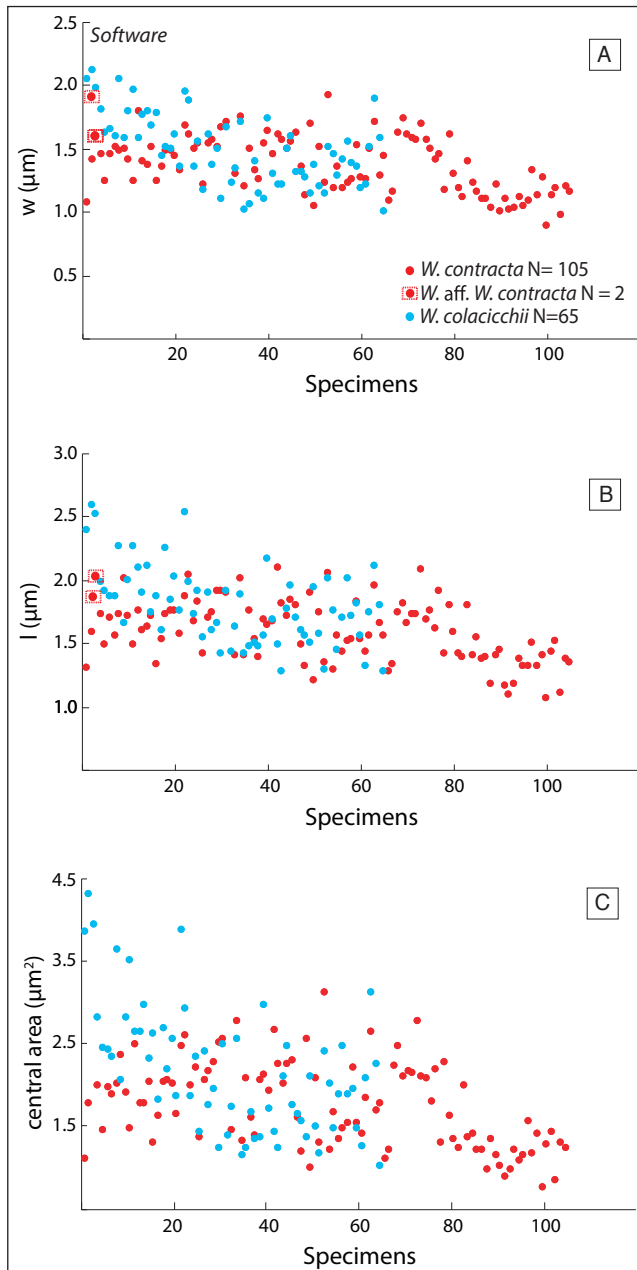


Fig. 4 – A) Variability of the central area width ( $w$ ) of *W. colacicchii* and *W. contracta* specimens. The specimens that belong to *W. aff. W. contracta* are highlighted. B) Variability of the central area length ( $l$ ) of *W. colacicchii* and *W. contracta* specimens. The two specimens that belong to *W. aff. W. contracta* are highlighted. C) Variability of the central area surface of *W. colacicchii* and *W. contracta* specimens.

Figure 3A illustrates the Pearson's correlation coefficient calculated for  $L$  and  $W$  of *W. colacicchii* and *W. contracta* specimens, showing a strong relationship for both taxa ( $R^2 = 0.85$  for both species). It is clear that the dimensional variability of the two taxa overlaps widely through the investigated interval (Fig. 3B), invalidating the use of this parameter for the taxonomic separation of *W. colacicchii* from *W. contracta*.

In the uppermost part of the Colle di Sogno section (from 118.3 m), a few *W. contracta* specimens bigger than  $7.5\ \mu\text{m}$  were observed. In previous papers (Cobianchi et al. 1992; Tiraboschi & Erba 2010; Ferreira et al. 2019; Fantasia et al. 2022), a *W. aff. W. contracta* group was used for specimens  $> 7\ \mu\text{m}$ . This dimensional distinction is contradictory relative to the original description of the species (Bown & Cooper 1989) and we, therefore, follow Erba (1990) in separating the specimens with  $L > 8.5\ \mu\text{m}$  as *W. aff. W. contracta* (Fig. 3).

As far as the size of the central area is concerned (Fig. 4), *W. colacicchii* and *W. contracta* specimens show largely overlapping dimensions, indicating that also this parameter is not species-diagnostic. We, therefore, considered the size of the central area relative to the coccolith size as quantified by the  $W/w$  ratio (Fig. 5) showing a clear separation of the two species: *W. colacicchii* specimens have a  $W/w$  ratio ranging from 2.2 to 3.4 and *W. contracta* specimens display a  $W/w$  ratio varying between 3.8 and 5.2. Pragmatically, we think that species attribution should be feasible/practicable during routine biostratigraphic investigation. For this reason, we measured a subset of *W. colacicchii* and *W. contracta* specimens using the micrometer scale inserted in the eyepieces of the polarizing microscope. Although inevitably the obtained measurements are less accurate, the results (Fig. 5B) are fully consistent with data obtained through image analyses (Fig. 5A) and confirm the reliability of the  $W/w$  ratio to separate *W. colacicchii* from *W. contracta* ( $W/w < 3.5$  for the former and  $W/w \geq 4.0$  for the latter). In Figure 5C the  $W/w$  ratio is plotted through the investigated interval: it is evident that the difference in  $W/w$  ratio for *W. colacicchii* and *W. contracta* specimens remains unchanged stratigraphically, allowing the unambiguous identification of the first occurrence of the two taxa (Fig. 2).

#### Morphometry of the *W. britannica* group

*W. britannica* was originally established as *Coccolithus britannicus* by Stradner (1963), subsequently Reinhardt (1964) included it in the genus *Watznaueria*. The taxon was described as an elliptical coccolith consisting of two closely appressed plates with an oval central opening transversally spanned by a short sturdy bridge. The illustrated holotype has  $L$  and  $W$  of  $7.8\ \mu\text{m}$  and  $6.1\ \mu\text{m}$ , respectively, as measured on the original drawing (Stradner 1963).

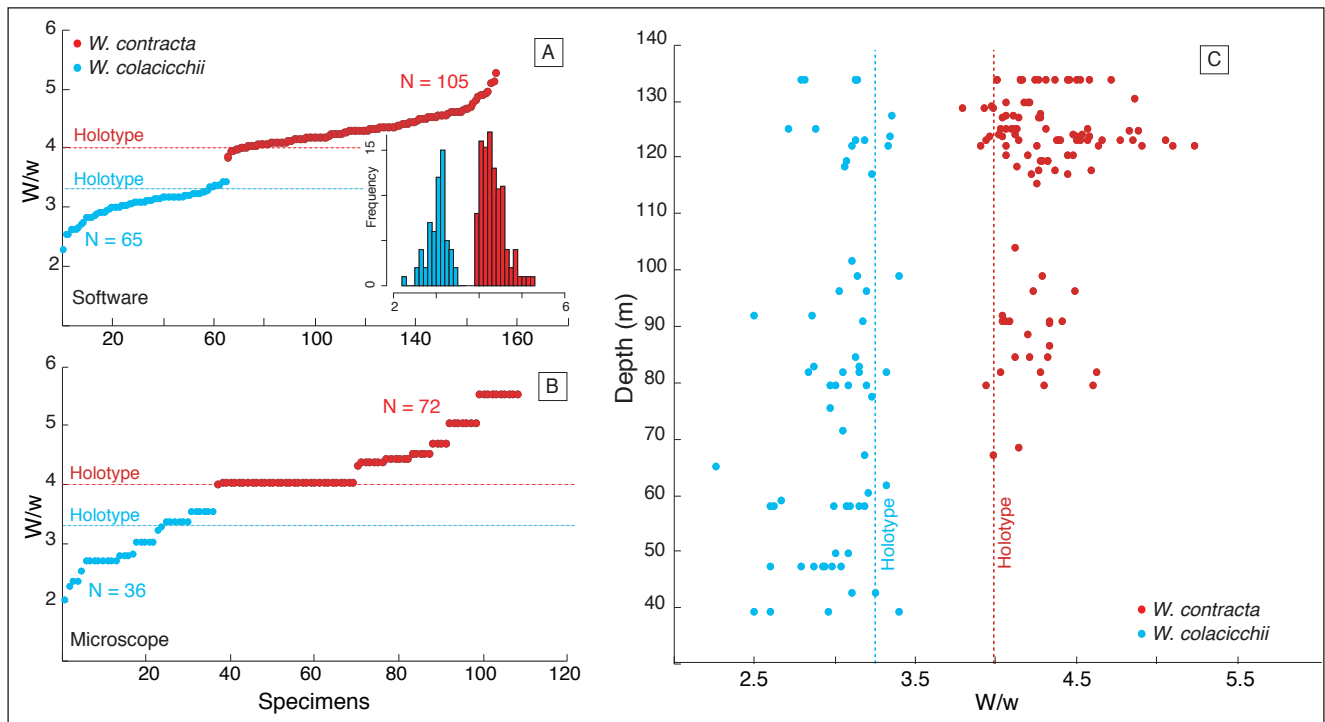


Fig. 5 – Variability of the coccolith width versus central area width =  $W/w$  ratio. A) The  $W/w$  ratio of *W. contracta*, and *W. colacicchii* were calculated for measurements obtained from photos using the software image]. The frequency distribution of  $W/w$  of *W. contracta* and *W. colacicchii* was calculated with the histogram function in R, considering every measured specimen. The size bins are 0.1 micrometers and the considered interval goes from 2 to 6 micrometers. B)  $W/w$  ratio of *W. contracta*, and *W. colacicchii* specimens measured at the light polarizing microscope. C) Stratigraphic distribution of the  $W/w$  in the Colle di Sogno section. The  $W/w$  ratio calculated for the holotypes of the two species are also reported.

In the Colle di Sogno section, specimens significantly different from the holotype were detected: they are smaller, thinner and generally more elliptical than the holotype. Moreover, under crossed nicols, these specimens show very low interference colors. In the literature, *W. britannica* specimens have been described with a wide dimensional range of coccolith  $L$  and  $W$ , and a variety of morphologies of the bridge spanning the central area. Pittet & Mattioli (2002) distinguished three *W. britannica* morphogroups based on  $L$ , namely  $< 6 \mu\text{m}$ ,  $6\text{--}8 \mu\text{m}$ ,  $> 8 \mu\text{m}$ . Oliver et al. (2004) applied a slightly different subdivision of *W. britannica* specimens with  $L < 5.5 \mu\text{m}$ ,  $5.5\text{--}8 \mu\text{m}$ ,  $> 8 \mu\text{m}$ . Tremolada et al. (2006) labelled the morphogroup with  $L < 5.5 \mu\text{m}$  as “small *W. britannica*”. Giraud et al. (2006, 2009) distinguished seven morphotypes (labelled as A, B, C, D, E, F and G) based on the general shape, coccolith size, central area dimensions and morphology of the bridge. The study by Giraud et al. (2006) is based on Oxfordian *W. britannica* specimens, and provide criteria partly overlapping thus not unambiguously applicable. Uncertainties, in particular, arise when considering morphotypes A, B and F,

as they all possess a button-shaped bridge and size ranges of  $L$  and  $W$ , as well as ellipticity ( $L/W$ ) partially overlapping. Moreover, as also stressed by Giraud et al. (2006), diagenesis may alter the original structure in the central area and, thus, the shape of the bridge is not a good diagnostic character.

Following the original description and illustration of Stradner (1963), during the biostratigraphic investigation we attributed the specimens with a coccolith  $L > 8 \mu\text{m}$  to *W. britannica* and grouped the specimens with a  $L < 8 \mu\text{m}$  into small *W. britannica* showing a coccolith  $L$  between 4 and 7  $\mu\text{m}$ . Then, a morphometric study of the *W. britannica* group was conducted on 51 samples. In each sample, 80 traverses (corresponding to 12,000 fields of views) were investigated: all encountered specimens (241) were photographed and coccolith  $L$  and  $W$ , as well as central area  $l$  and  $w$  were measured.

Figure 6 illustrates the variability of  $L$  and  $W$  of *W. britannica* coccoliths. The Pearson coefficient shows a positive correlation between  $L$  and  $W$  for small *W. britannica* specimens ( $R^2 = 0.69$ ) but not for *W. britannica* specimens, possibly because of the limited number of individuals. The size variability

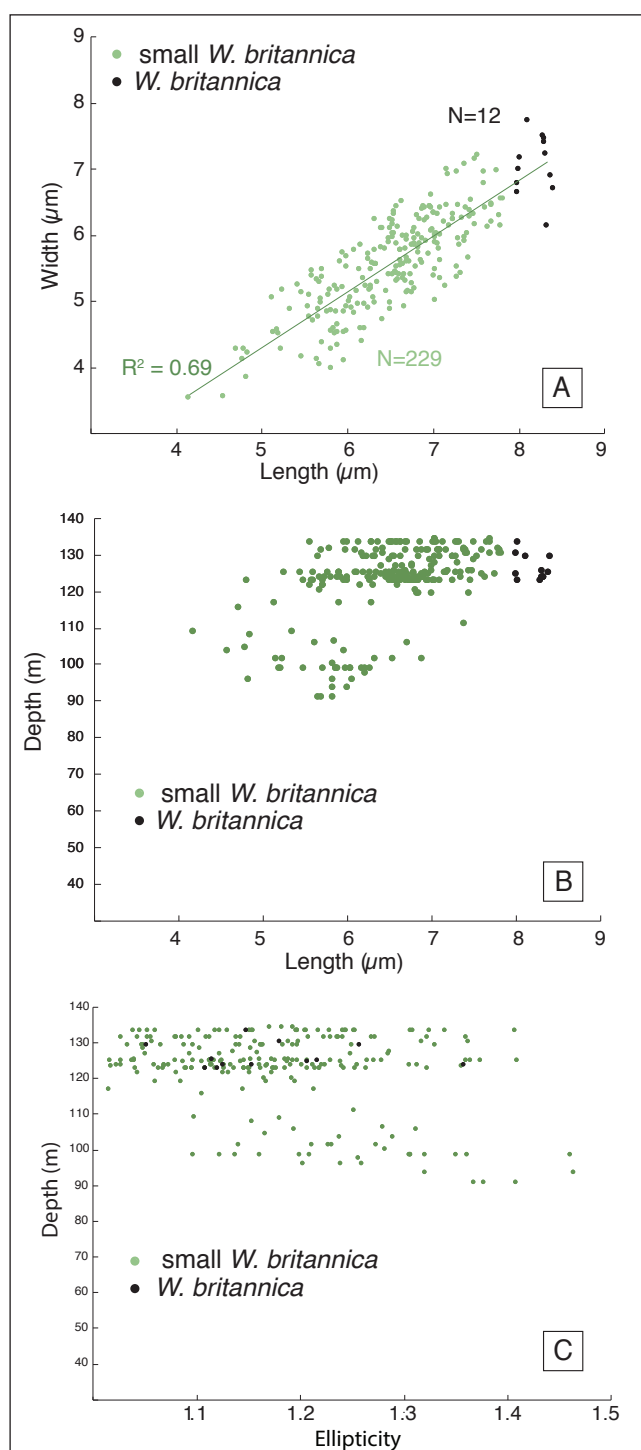


Fig. 6 – A) Scatter plots of *W. britannica* and small *W. britannica* coccolith length versus width with the coefficient determinations ( $r^2$ ). The number of measurements is also given (N). B) Length of the distal shield of *W. britannica* and small *W. britannica* specimens versus depth. C. Ellipticity ( $e = L/W$ ) of the distal shield of *W. britannica* and small *W. britannica* specimens versus depth.

in the studied interval (Fig. 6B) shows that small *W. britannica* coccoliths increase in L upwards and that *W. britannica* specimens occur only in the uppermost part of the studied section.

The ellipticity ( $e = L/W$  ratio) shows the occurrence of less elliptical specimens (decreasing  $e$  values) in the upper part of the studied interval (Fig. 6C). This is the result of faster increasing  $W$  relative to  $L$ , leading to overall less elliptical coccoliths.

The three types of bridge morphologies described by Giraud et al. (2006), namely button, bar and rhombohedral, were observed in both small *W. britannica* and *W. britannica* specimens. Out of 241 specimens 221 display a central area almost entirely filled by a button-shaped bridge, 15 are characterized by a rhombohedral bridge and only 5 specimens have a partially open central area with an oval-shaped bridge. Our results document rhombohedral and oval bridges exclusively in the uppermost part of the section and generally characteristic of larger specimens ( $> 6.5 \mu\text{m}$ ).

In the investigated interval, *Watznaueria* specimens with a very small central area spanned by a bridge consisting of two small buttons that are optically discontinuous relative to the coccolith rim were observed. This bridge ultrastructure is unambiguously distinctive from other typologies and found in specimens characterized by a high  $W/w$  ratio ( $> 4.7$ ). Similar *Watznaueria* specimens have not been documented in previous works and we define here a new species (see below).

#### *Implications for taxonomy of Watznaueria*

Morphometric analyses turned out to be diagnostic to unambiguously separate *Watznaueria* taxa based on parameters summarized in Figure 7. Specifically, *W. colacicchii* and *W. contracta* are distinguished on the basis of the  $W/w$  ratio, *W. gaetanii* is characterized by the bridge ultrastructure and *W. britannica* is discriminated by the coccolith size. Accordingly, the taxonomy of *Watznaueria* species is revised below.

#### Genus *Watznaueria* Reinhardt (1964)

##### *Watznaueria britannica* subsp. *minor* Erba n. subsp.

Plate 2, Figs. 7 - 18

**Etymology:** the name derives from the diagnostic small size of the coccoliths relative to *Watznaueria britannica* subsp. *britannica*.

**Diagnosis:** a subspecies of *W. britannica* comprising elliptical, small ( $L < 7.6 \mu\text{m}$ ) and thin coccoliths with low interference colours (grey to white).

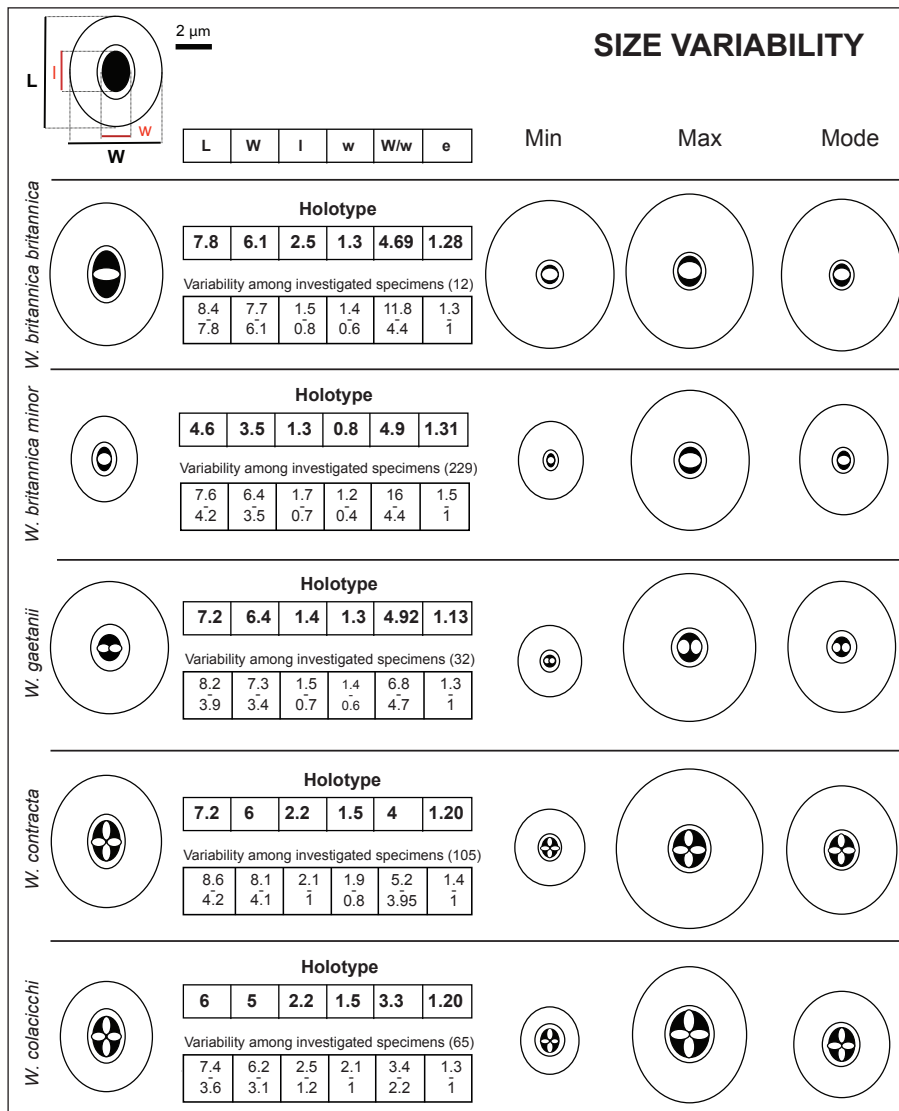


Fig. 7 – Summary of sizes of investigated parameters in the holotypes and the variability of the measured specimens for individual *Watznaueria* taxa. Numbers of specimens measured (N) are provided. On the left, the holotype is figured while on right the minimum, maximum and mode sizes are illustrated for each taxa.

Specimens are observed to possess a wide variability of bridge morphology (i.e., button, rhombohedral and oval). An oval-shaped bridge is only observed in specimens with a relatively larger central area while the other bridge shapes are characteristic of a very small central area.

**Remarks:** morphometric analyses separate specimens with L of 4.2 – 7.6 µm, W of 3.5 – 6.4 µm, ellipticity of 1.03 – 1.5. The illustration of Reinhardt (1964; Plate 2, Fig. 3) pertains a coccolith with L = 6 µm which is therefore referable to *Watznaueria britannica* subsp. *minor*.

**Differentiation:** *Watznaueria britannica* subsp. *minor* differs from *Watznaueria britannica* subsp. *britannica* for its smaller size (L < 7.6 µm; average L = 6.5 µm). Typically, coccoliths of *Watznaueria britannica* subsp. *minor* show lower interference colours (grey to white) relative to coccoliths of *Watznaueria britannica* subsp. *britannica* (yellow to orange).

**Stratigraphic range:** *Watznaueria britannica* subsp. *minor* was first observed in the middle Aalenian consistently with the stratigraphic position provided by Ferreira et al. (2019) for the FO of *W. britannica* morphotype A.

**Holotype:** Plate 2, Figs 7-8. Holotype L = 4.6 µm; W = 3.5 µm.

**Type locality:** Colle di Sogno (Northern Italy).

**Type level:** Jurassic, middle-late Aalenian.

**Depository:** Department of Earth Sciences “Ardito Desio” of Milan (Reference MPUM 12568).

***Watznaueria britannica* subsp. *britannica***  
**Stradner (1963) Reinhardt (1964) emend. Erba**

Plate 2, Figs. 1 - 6

**Basionym:**

1963 *Coccolithus britannicus* Stradner, p. 10, figs. 10-10a.

**Reference:**

1964 *Watznaueria britannica* Stradner; Reinhardt, pp. 753-755.

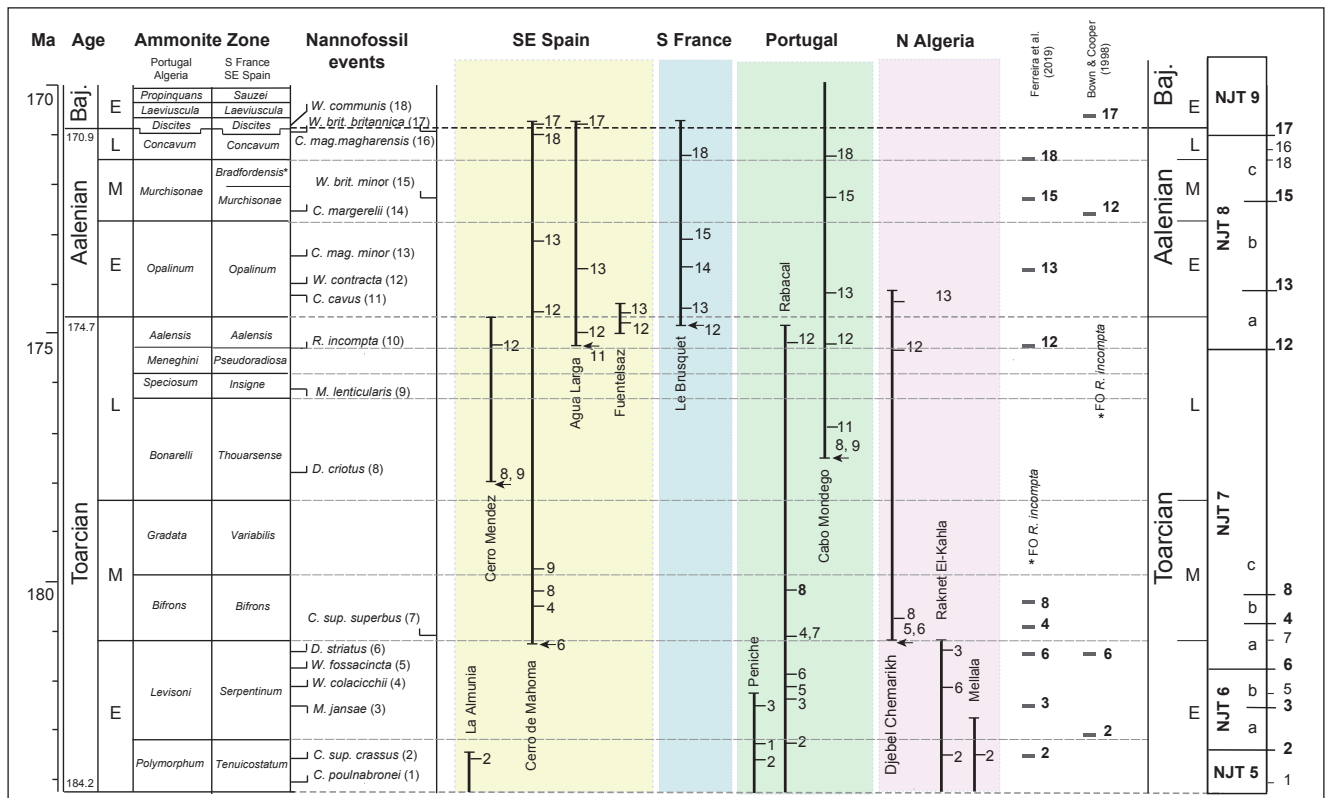


Fig. 8 – The nannofossil events in the zonation of Mattioli & Erba (1999) implemented with biohorizons recognized in the Colle di Sogno section are compared with ammonite-calibrated events documented in Mediterranean sections. A comparison with the Lusitanian Basin (Ferreira et al. 2019) and Boreal (Bown & Cooper 1998) zonation schemes is also reported. On the right, the summary of nannofossil events, zones and subzones and the ammonite-based chronostratigraphy.

**Description:** This subspecies comprises coccoliths with  $L > 7.8 \mu\text{m}$ , consistently with the original description of Stradner (1964). In the studied interval the coccolith size variability is:  $L 7.8 - 8.4 \mu\text{m}$ ,  $W 6.1 - 7.7 \mu\text{m}$ . In the light microscope under crossed nicols, specimens of *W. britannica* subsp. *britannica* show relatively high interference colours (yellow to orange). The small central area is open and spanned by a button, rhombohedral or oval bridge.

**Differentiation:** Our morphometric analyses allowed the separation of *W. britannica* subsp. *britannica* from *W. britannica* subsp. *minor* based on the coccolith  $L > 7.8 \mu\text{m}$ .

**Stratigraphic range:** the FO of *W. britannica* subsp. *britannica* was found in the uppermost Aalenian, at a stratigraphic level consistent with that reported in the zonal scheme of Mattioli & Erba (1999) for *W. britannica*.

**Holotype:** Stradner (1963, figs. 10-10a). Holotype  $L: 7.8 \mu\text{m}$ .

### *Watznaueria colacicchii* Mattioli (1996)

**Original diagnosis:** A broadly elliptical to sub-circular species of the genus *Watznaueria*, with a reduced central area crossed by a system of bars forming a cross, aligned with the axes of the coccolith (Mattioli, 1996).

**Remarks:** Based on the morphometric analyses conducted here, this species is typified by a  $W/w$  ratio  $< 3.5$  that unambiguously separates *W. colacicchii* from *W. contracta*.

**Stratigraphic range:** The FO of this species was detected in the middle Toarcian at Colle di Sogno, at a stratigraphic level consistent with that proposed in the zonal scheme of Ferreira et al. (2019). Mattioli & Erba (1999), instead, placed this event in the upper lower Toarcian.

### *Watznaueria contracta* Bown & Cooper (1989) Cobianchi et al. (1992)

**Original diagnosis:** A species of *Lotharingius* with a very small central area almost entirely filled by cross bars orientated along the principal axes of the ellipse; few or no lateral bars (Bown & Cooper 1989). Cobianchi et al. (1992) moved the species within the genus *Watznaueria*.

**Remarks:** Based on the morphometric analyses conducted here, this species is characterized by a W/w ratio > 4 that unambiguously separates *W. contracta* from *W. colacicchii*. In the present work the morphotype labelled as *W. aff. W. contracta* includes the specimens with a length of the distal shield L > 8.5 µm following Erba (1990).

**Stratigraphic range:** The FO of *W. contracta* was found before the FO of *C. magharensis minor* in the uppermost Toarcian at a stratigraphic level consistent with the zonal scheme of Ferreira et al. (2019). At Colle di Sogno, the *W. aff. W. contracta* group was identified in the lowermost Bajocian consistently with the scheme of Mattioli & Erba (1999).

### *Watznaueria gaetanii* Erba n. sp. (Plate 2, micrographs 19-32)

**Etimology:** honor of the late Maurizio Gaetani, former full professor at the Dept. of Earth Sciences, University of Milan (Italy), geologist and stratigrapher (1940-2017).

**Diagnosis:** species of *Watznaueria* with a small central area spanned by a bridge consisting of two button-like elements aligned along the minor axis of the ellipse.

**Description:** relatively large coccolith with a typical watznaueriacean rim and a very small central area spanned by a bridge consisting of two button-shaped elements aligned along the minor axis of the ellipse. The two bridge elements display optical discontinuity relative to the inner cycle of the coccolith rim.

**Remarks:** on available data, the coccolith L and W are 3.9 – 8.2 µm and 3.4 – 7.4 µm, respectively, with an ellipticity (e) of 1.05 – 1.35. The central area l and w are 0.7 – 1.6 µm and 0.6 – 1.5 µm, respectively. The L/l and the W/w ratios range between 4.0 – 6.8 and 4.7 – 6.9, respectively.

**Stratigraphic range:** the FO of *W. gaetanii* was detected in the middle Aalenian, slightly after the FO of *W. contracta*.

**Differentiation:** *Watznaueria gaetanii* differs

from the other species of the genus for its peculiar bridge.

**Holotype:** Plate 2, 19-22. Holotype L: 7.2 µm; W: 6.4 µm; e: 1.13; l: 1.4 µm; w: 1.3 µm; L/l: 5.1; W/w: 5.1.

**Type locality:** Colle di Sogno, Lombardy Basin (Southern Alps, Northern Italy)

**Type level:** Jurassic, middle Aalenian

**Depository:** Dept. of Earth Sciences “Ardito Desio”, Univ. of Milan (Reference MPUM n. 12537)

### PLATE 1

- Figs. 1-2 – *C. magharensis magharensis* top view (TV), 1) cross-polarized light, 2) quartz lamina, sample JET (131.75 m).  
 Figs. 3-4 – *C. magharensis magharensis* top view (TV), 3) cross-polarized light, 4) quartz lamina, sample JET (122.80 m).  
 Figs. 5-6 – *C. magharensis minor* top view (TV), 5) cross-polarized light, 6) quartz lamina, sample JET (123.75 m).  
 Figs. 7-8 – *C. magharensis minor* side view (SV), 7) cross-polarized light, 8) quartz lamina, sample CSS#189 (98.75 m).  
 Figs. 9-10 – *C. superbus crassus* side view (SV), 9) cross-polarized light, 10) quartz lamina, sample CSS#96 (24.35 m).  
 Figs. 11-12 – *C. superbus superbus* side view (DV), 11) cross-polarized light, 12) quartz lamina, sample CSS#189 (98.75 m).  
 Figs. 13-14 – *C. crassus*, 13) cross-polarized light, 14) quartz lamina, sample CSS#173 (90.85 m).  
 Figs. 15-16 – *D. criotus*, 15) cross-polarized light, 16) quartz lamina, sample CSS#173 (90.85 m).  
 Figs. 17-18 – *D. ignotus*, 17) cross-polarized light, 18) quartz lamina, sample CSS#221 (123.30 m).  
 Figs. 19-20 – *D. striatus*, 19) cross-polarized light, 20) quartz lamina, sample CSS#119 (52.40 m).  
 Figs. 21-22 – *L. crucicentralis*, 21) cross-polarized light, 22) quartz lamina, sample CSS#189 (98.75 m).  
 Figs. 23-24 – *L. frodoi*, 23) cross-polarized light, 24) quartz lamina, sample JET#101 (32.75 m).  
 Figs. 25-26 – *L. bauffii*, 25) cross-polarized light, 26) quartz lamina, sample CSS#90 (19.90 m).  
 Figs. 27-28 – *M. lenticularis*, 27) cross-polarized light, 28) quartz lamina, sample CSS#94 (21.95 m).  
 Figs. 29-30 – *R. incompta*, 29) cross-polarized light, 30) quartz lamina, sample CSS#139 (67.25 m).  
 Figs. 31-32 – *S. punctulata*, 31) cross-polarized light, 32) quartz lamina, sample CSS#93 (20.25).  
 Figs. 33-34 – “encrusted” *S. punctulata*, 33) cross-polarized light, 34) quartz lamina, sample JET#181 (94.60 m).  
 Figs. 35-36 – *T. sullivanii*, 35) cross-polarized light, 36) quartz lamina, sample CSS#189 (98.75 m).  
 Scale bars represent 2 µm.

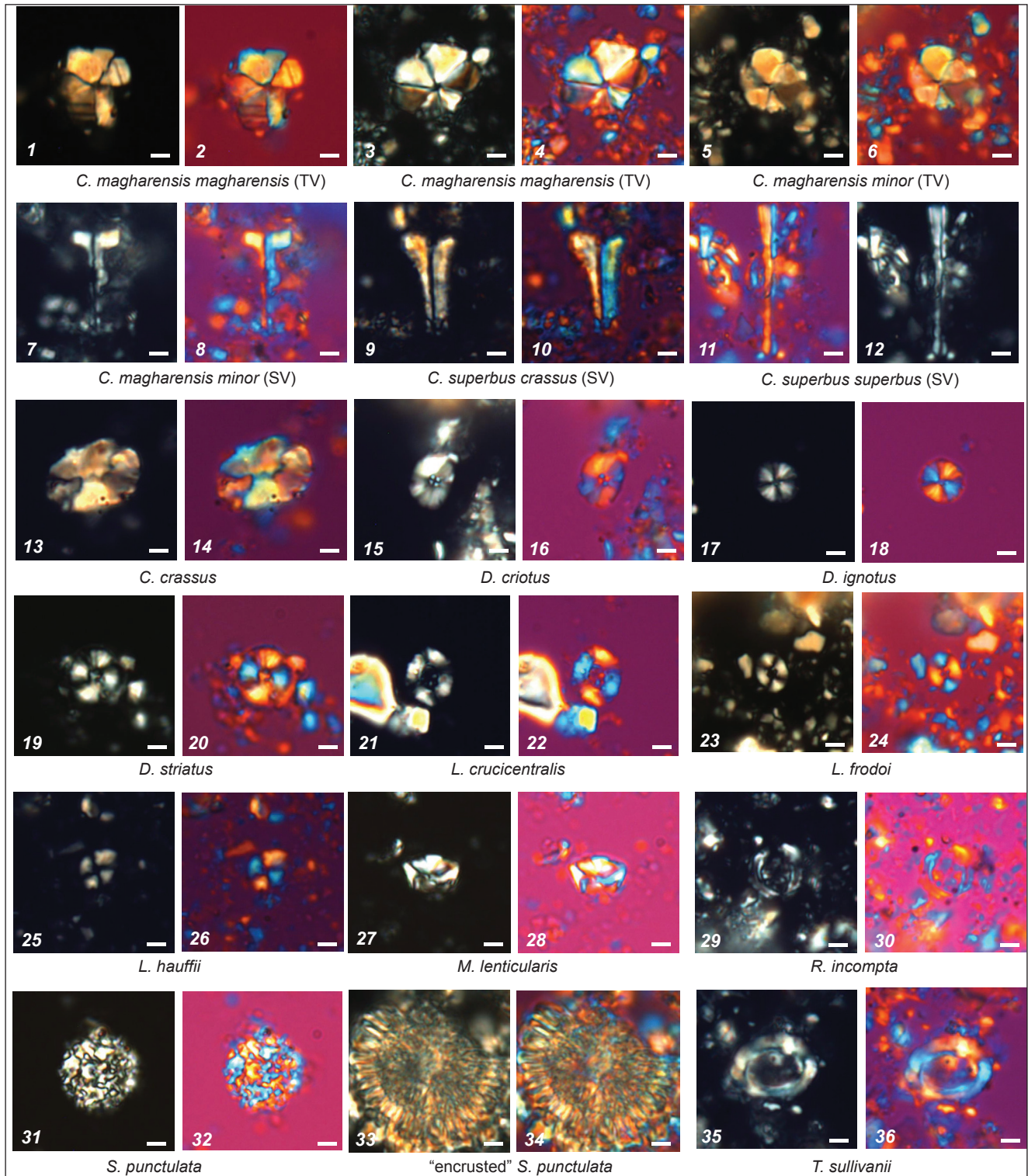


PLATE 1

### Biostratigraphy of the Colle di Sogno section

Biostratigraphic investigation of the lower part of the section, from -11.97 m to 19.14 m, covering the uppermost Domaro Limestone Fm. and the lowermost Lithozone 1 of the Sogno Fm., was

previously carried out by Casellato & Erba (2015). We revisited this interval to apply the updated taxonomy of the genus *Carinolithus* (Visentin et al. 2021a). The new analyses confirmed most events (and their m level) documented by Casellato & Erba (2015) with the exception of the FO of *L. sigillatus*

in the topmost sample from the Domaro Limestone Fm. (-0.15 m) and the FO of *C. superbus crassus* (*C. superbus* in Casellato & Erba 2015) at 8.4 m (35 cm below the record of Casellato & Erba 2015). The base of the NJT6 Zone is thus placed accordingly (Fig. 2).

The last occurrence (LO) of *Mitrolithus jansae* at 14.05 m was used to separate the NJT6a and NJT6b Subzones as proposed by Ferreira et al. (2019) and recently applied in the Tethyan domain (Visentin & Erba 2021b). The FO of *Discorhabdus striatus* at 26.75 m defines the NJT6/NJT7 zonal boundary. Within the NJT7 Zone, the FOs of *C. superbus superbus* (31.30 m), *Watznaueria colacicchii* (39.15 m) and *Discorhabdus criotus* (47.30 m) were detected. Also, in the upper part of the NJT7 Zone the LOs of *Mitrolithus lenticularis* and *Crepidolithus cavus* were observed at 52.40 m and 65.05 m, respectively (Fig. 2).

In the Colle di Sogno section, *Retecapsa incompta* is extremely sporadic (see range chart in Appendix 2) and, thus, cannot be used as zonal marker for the base of the NJT8 Zone. The FO of *Watznaueria contracta* was detected at 66.95 m and is used here to identify the NJT8 Zone. In the lowermost part of this zone *Carinolithus magharensis minor* (top view = TV) first occurs at 69.65 m. Other biohorizons detected in the NJT8 Zone comprise the FOs of *Watznaueria gaetanii* at 81.80 m, *W. britannica minor* at 90.85 m and *W. communis* at 96.05 m (Fig. 2). Specimens of *Cyclagelosphaera margerelii* were not observed in the Colle di Sogno section.

The FO of *Watznaueria britannica britannica* defines the base of the NJT9 Zone at 122.80 m. In the same sample the FO of *Carinolithus magharensis* (IV) was observed. Within the NJT9 Zone the FOs of *W. aff. W. contracta* and *W. aff. W. manivittiae* were detected at 126.80 m and 129.40 m, respectively. The uppermost investigated sample at 136 m is still included in the NJT9 Zone due to the absence of *Watznaueria manivittiae*, the zonal marker identifying the base of the NJT10 Zone.

The distribution of calcareous nannofossils in the Colle di Sogno section is documented in the range chart of Appendix 2, and the marker species are illustrated in Plates 1 and 2. Nannofossil assemblages characterizing the NJT6 Zone mainly consist of genus *Lotharingius* (*L. hauffii* is the dominant species, followed by *L. frodoi* and *L. sigillatus*). Other frequent-common genera are *Schizosphaerella*, *Calyculus*, *Carinolithus* and *Crepidolithus* (essentially *C.*

*crassus*). Within the NJT7 Zone a decrease in abundance of genera *Lotharingius*, *Calyculus*, *Carinolithus*, *Crepidolithus* and *Biscutum* and a concomitant increase of *Discorhabdus* is observed whereas *Schizosphaerella* remains a common component of the assemblages. The nannofloral composition of the NJT8 Zone is similar to that of the NJT 7 Zone with a progressive increase in abundance of the genus *Watznaueria*. The NJT9 Zone is characterized by common *Schizosphaerella* and frequent *Watznaueria*. Other frequent genera

---

PLATE 2

- Figs. 1-2 – *W. britannica britannica* (button-shaped bridge), 1) cross-polarized light, 2) quartz lamina, sample JET 122.8 (122.80 m).  
 Figs. 3-4 – *W. britannica britannica* (oval-shaped bridge), 3) cross-polarized light, 4) quartz lamina, sample JET 123.75 (123.75 m).  
 Figs. 5-6 – *W. britannica britannica* (rhombohedral-shaped bridge), 5) cross-polarized light, 6) quartz lamina, sample JET 130.19 (130.19 m).  
 Figs. 7-8 – *W. britannica minor* (button-shaped bridge), 7) cross-polarized light, 8) quartz lamina, sample JET 103.7 (103.70 m).  
 Figs. 9-10 – *W. britannica minor* (oval-shaped bridge), 9) cross-polarized light, 10) quartz lamina, sample JET 122.8 (122.8 m).  
 Figs. 11-12 – *W. britannica minor* (rhombohedral-shaped bridge), 11) cross-polarized light, 12) quartz lamina, sample CSS#227 (133.55 m).  
 Figs. 13-14 – *W. britannica minor* (button-shaped bridge), 13) cross-polarized light, 14) quartz lamina, sample CSS#193 (133.55 m) 101.4 m (CSS193).  
 Figs. 15-16 – *W. britannica minor* (button-shaped bridge), 15) cross-polarized light, 16) quartz lamina, sample CSS#193 (101.4 m).  
 Figs. 17-18 – *W. britannica minor* (button-shaped bridge), 17) cross-polarized light, 18) quartz lamina, sample JET 122.8 (122.80 m).  
 Figs. 19-20 – *W. colacicchii*, 19) cross-polarized light, 20) quartz lamina, sample JET 122.8 (122.80 m).  
 Figs. 21-22 – *W. contracta*, 21) cross-polarized light, 22) quartz lamina, sample JET (121.70 m).  
 Figs. 23-24 – *W. aff. W. contracta*, 23) cross-polarized light, 24) quartz lamina, sample CSS#227 (133.55 m).  
 Figs. 25-28 – *W. gaetanii*, 25, 27) cross-polarized light, 26, 28) quartz lamina, sample JET (131.40 m).  
 Figs. 29-30 – *W. gaetanii*, 29) cross-polarized light, 30) quartz lamina, sample JET (121.70 m).  
 Figs. 31-32 – *W. gaetanii*, 31) cross-polarized light, 32) quartz lamina, sample JET (121.70 m).  
 Figs. 33-34 – *W. gaetanii*, 33) cross-polarized light, 34) quartz lamina, sample JET (124.95 m).  
 Figs. 35-36 – *W. gaetanii*, 35) cross-polarized light, 36) quartz lamina, sample JET (124.95 m).  
 Figs. 37-38 – *W. gaetanii*, 37) cross-polarized light, 38) quartz lamina, sample JET (124.95 m).  
 Figs. 39-40 – *W. communis*, 39) cross-polarized light, 40) quartz lamina, sample CSS#200 (106.35 m).  
 Figs. 41-42 – *W. fossacincta*, 41) cross-polarized light, 42) quartz lamina, sample JET (124.60 m).  
 Scale bars represent 2 µm.

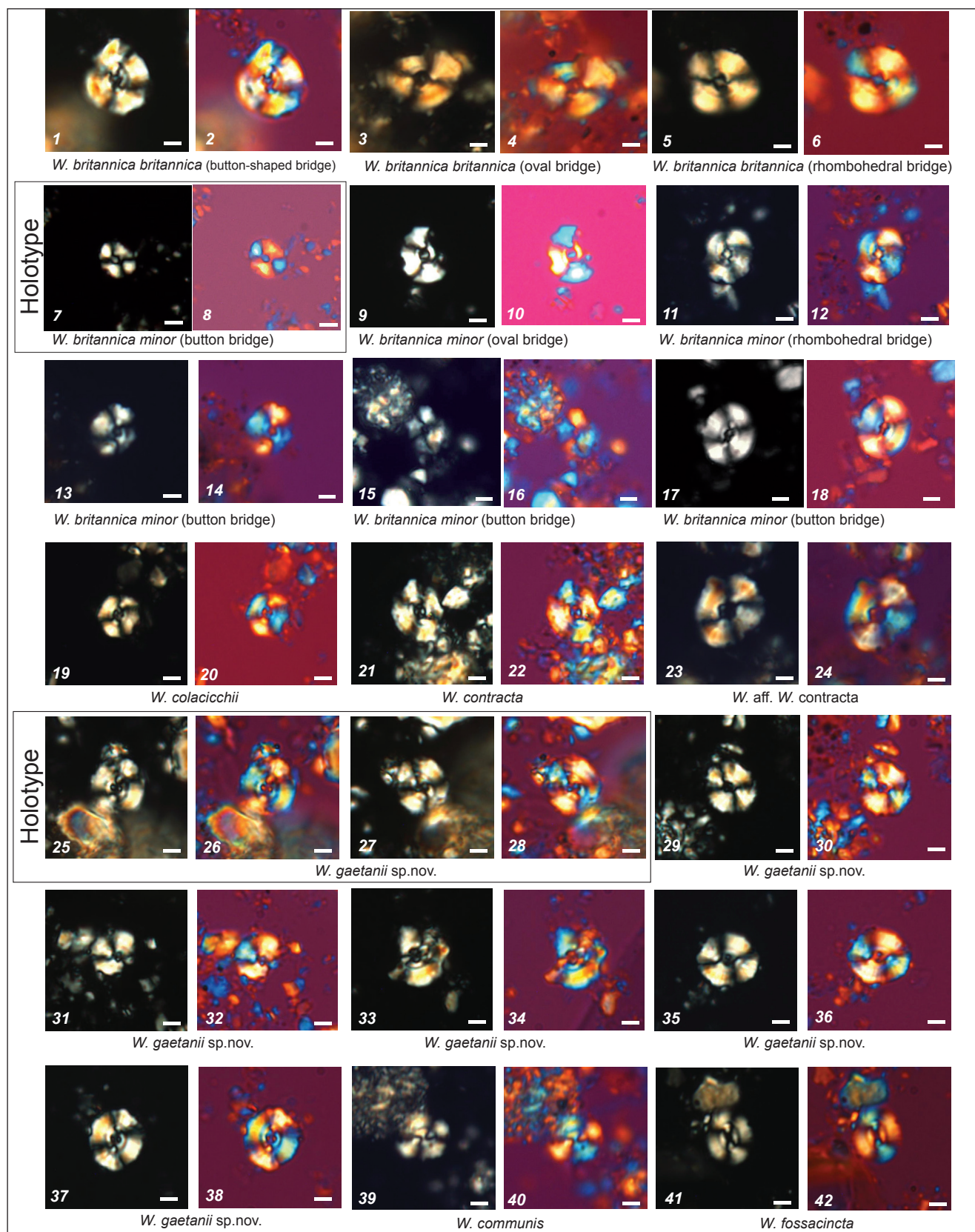


PLATE 2

are *Discorbabodus* and *Carinolithus*. A further decrease of the genus *Lotharingius* occurs whereas *Biscutum* and *Calyculus* become extremely rare and sporadic.

Through the studied section, genera *Mitrolithus*, *Turbabodus*, *Triscutum*, *Bussonius*, *Orthogonoides*, *Diazomatolithus* and *Retecapsa* are rare to extremely rare.

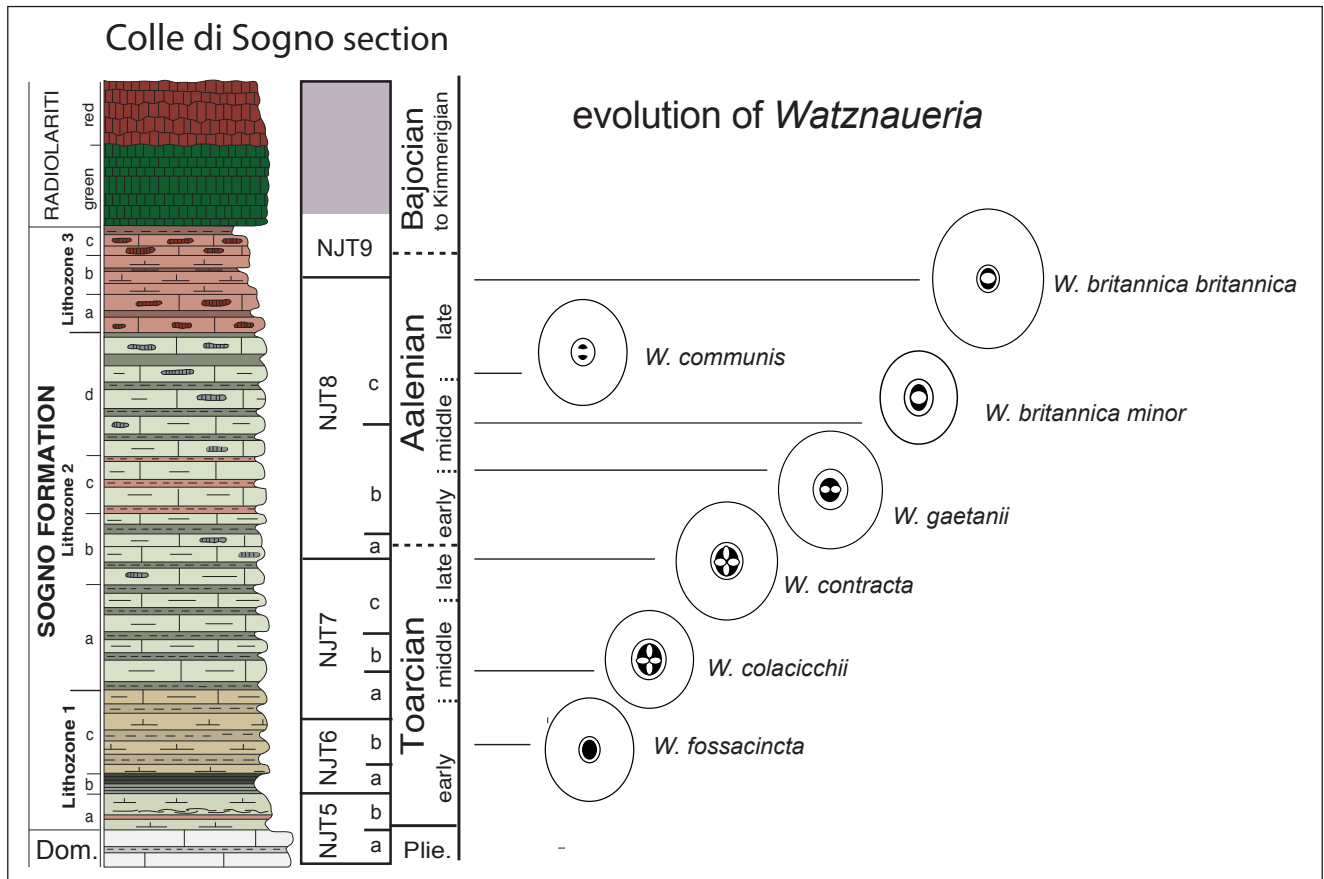


Fig. 9 – Stratigraphic distribution of *Watznaueria* taxa in the Colle di Sogno section.

## COMPARISON WITH THE BIOZONATION SCHEMES AND PUBLISHED LITERATURE

The biozonation of Mattioli & Erba (1999) represents the Jurassic reference scheme for Mediterranean sections (Italy, North and East Spain, South France, Hungary, Greece) and was applied in many studies in the last two decades. Recently, Ferreira et al. (2019) published a synthesis of events based on sections from the Lusitanian Basin representing the intersection area between the Boreal Realm and the Tethys Ocean, thus providing nanofossil data for a comparison between the Boreal (Bown & Cooper 1998) and Tethyan (Mattioli & Erba 1999) events and zones.

Casellato & Erba (2015) discussed lower Toarcian nanofossil events calibrated against ammonite biostratigraphy and/or C isotopic chemostratigraphy. Here, we extend the analysis to the middle Toarcian - lower Bajocian nanofossil events calibrated with ammonite zones in France, Spain, Portugal and Algeria (Cresta et al. 2001; Aguado et al. 2008; Sandoval et al. 2008, 2012; Molina et al. 2018;

Ferreira et al. 2019; Menini et al. 2019; Baghli et al. 2022; Fantasia et al. 2022), as synthesized in Figure 8. In the following section, we discuss the events proposed by Mattioli & Erba (1999) as zonal and subzonal markers implemented with additional datums recognized in recent papers.

The FO of *C. poulabronei* was reported only at Peniche from the topmost part of the polymorphum Ammonite Zone (AZ).

The FO of *C. superbus crassus* was recognized in all sections consistently in the upper part of the tenuicostatum/polymorphum AZ. The revised taxonomy of Visentin et al. (2021a) was applied to the N Algeria sections (Baghli et al. 2022), whereas in other studies the FO of *C. superbus* was reported.

The LO of *M. jansae* is documented in the middle of the serpentinum/levisoni AZ, with the only exception of the Raknet El-Kahla section (Baghli et al. 2022) where this event was found in the upper part of this ammonite zone. Recent investigations confirm that the LO of *M. jansae* is a reliable and reproducible event, as assessed by Ferreira et al. (2019).

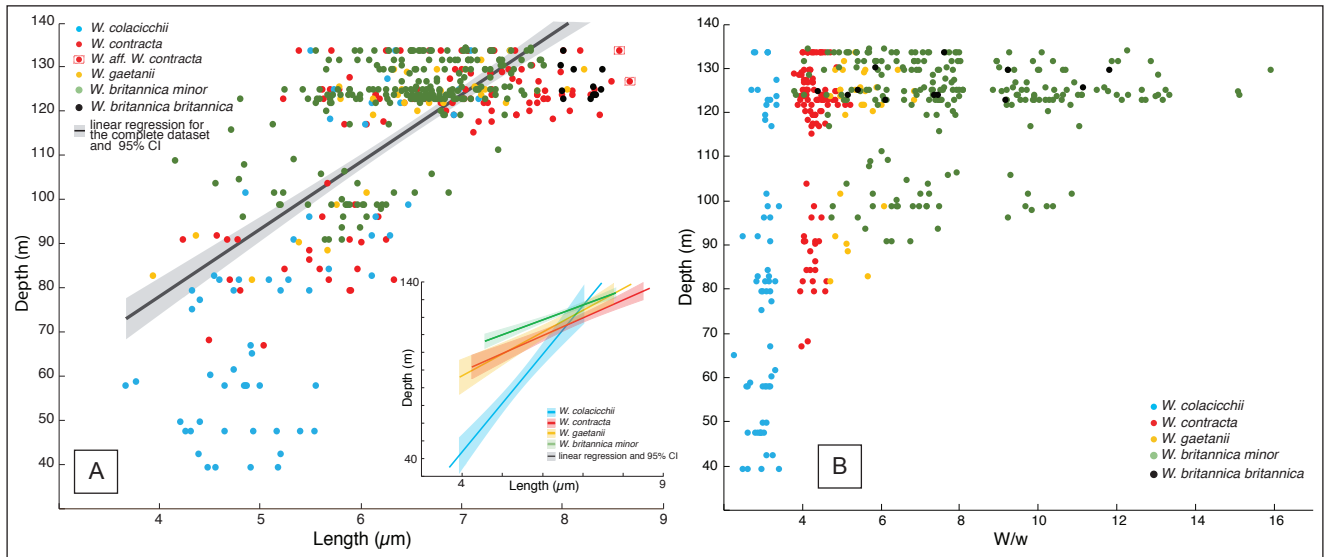


Fig. 10 – A) Variability of the distal shield length of *W. contracta*, *W. aff. W. contracta*, *W. colacicchii*, *W. gaetanii*, *W. britannica minor*, and *W. britannica britannica* versus depth; the linear regression of the complete dataset is also represented with the interval of confidence (95%). In the box the linear regressions of the length of the various species are illustrated separately with the interval of confidence (95%) for each line. B) Variability of the W/w of *W. contracta*, *W. aff. W. contracta*, *W. colacicchii*, *W. gaetanii*, *W. britannica minor*, and *W. britannica britannica* versus depth.

Unlike the zonation of Mattioli & Erba (1999), the FO of *W. colacicchii* was recognized in the bifrons AZ consistently with the datum in the zonation of Ferreira et al. (2019), although at slightly different stratigraphic levels. At Rabacal this event is reported from the base of the bifrons AZ (Ferreira et al. 2019), whereas in the Cerro de Mahoma section it is documented from the middle part of the bifrons AZ (Sandoval et al. 2008).

The FO of *W. fossacincta* was used only at Rabacal in the middle part of the levisonii AZ (Ferreira et al. 2019), similarly to the Mattioli & Erba (1999) zonation.

The FO of *D. striatus* was recognized in all sections within the serpentinum/levisonii AZ, at slightly older levels relative to the zonations of Mattioli & Erba (1999) and Ferreira et al. (2019).

The FO of *C. superbus superbus* was recognized at Rabacal in the lowermost bifrons AZ (reported as *C. superbus* “thin and long” in Ferreira et al. 2019). This is a new additional event proved to be reproducible.

The FO of *D. criotus* is documented in the middle part of the bifrons AZ in all section suggesting an age older than that reported by Mattioli & Erba (1999) and consistent with Ferreira et al. (2019).

The LO of *M. lenticularis* was not used in the analyzed biostratigraphies (Fig. 7) suggesting that this event is not reliable.

The FO of *R. incompta* was not adopted as an event because this taxon is extremely rare in all analyzed sections. Thus, the datum proposed by Mattioli & Erba (1999) to place the base of the NJT 8 nannofossil zone cannot be used in Tethyan sections. The FO of *R. incompta* is calibrated to the middle Toarcian (gradata AZ) in Portugal (Ferreira et al. 2019) and to the and late Toarcian (levesquei AZ) in the Boreal realm (Bown & Cooper 1998). We conclude that this datum is problematic and should not be used.

The LO of *C. cavus* was not used in the analyzed biostratigraphic works suggesting that this event is not reliable.

The FO of *W. contracta* was found in all sections within the aalensis AZ, with the only exception of the Cerro de Mahoma section where this event was found in the lowermost opalinum AZ (Sandoval et al. 2008) and the Djebel Chemarikh section where it is calibrated to the top of the meneghini AZ (Baghli et al. 2022). These data are different from the age attribution of Mattioli & Erba (1999) to the opalinum AZ and more consistent with Ferreira et al. (2019) who placed the FO of *W. contracta* at the base of the aalensis AZ. We suggest here to use the FO of *W. contracta* to place the base of the NJT 8 nannofossil Zone.

The FO of *C. magharensis minor* (reported as *C. magharensis* or *H. magharensis*) was recognized in all sections in the opalinum AZ. This datum results

to be very reliable and confirms the previous age assignment of Mattioli & Erba (1999) and Ferreira et al. (2019).

The FO of *C. margerelii* was reported only at Le Brusquet in the opalinum AZ (Fantasia et al. 2022). This taxon is absent in all other sections and not observed at Colle di Sogno. This event was not included in the zonation of Ferreira et al. (2019) and we conclude that it is not a reproducible marker in the Aalenian-lower Bajocian interval.

The FO of *W. britannica minor* is here equated to the FO of the *W. britannica* morphotype A of Giraud et al. (2006) (see discussion in the taxonomic chapter). This event was reported at Le Brusquet and Cabo Mondego in the upper part of the opalinum AZ and the middle part of the murchisoniae AZ, respectively. Ferreira et al. (2019) used the FO of *W. britannica* morphotype A to place the base of the NJT 9 nannofossil zone in the middle murchisoniae AZ. We suggest to use the FO of *W. britannica minor* as an additional event within the NJT 8 nannofossil zone.

The FO of *C. magharensis magharensis* was detected at Colle di Sogno in the same sample with the FO of *W. britannica britannica*. *C. magharensis magharensis* was defined by Visentin et al. (2021a) and not used in the analyzed works.

The FO of *W. britannica britannica* was reported at Cerro de Mahoma and Agua Larga (as *W. britannica*, Sandoval et al. 2008) in the lowermost discites AZ. The definition is specifically discussed and applied to specimens with the diagnostic features of the *W. britannica* holotype. Thus, the same criteria used here as well as by Mattioli & Erba (1999) were adopted. We consider the FO of *W. britannica britannica* a reliable event to place the base of the NJT 9 nannofossil zone in the latest Aalenian as proposed by Mattioli & Erba (1999).

The FO of *W. communis* was documented in the concavum AZ at Cerro de Mahoma (Sandoval et al., 2008), Le Brusquet (Fantasia et al. 2022) and Cabo Mondego (Ferreira et al. 2019). This is different from the age attribution of Mattioli & Erba (1999) who placed this event in the discites AZ. In the zonation of the Lusitanian Basin, Ferreira et al. (2019) reported this event at the base of the concavum AZ.

The critical evaluation of nannofossil biohorizons calibrated against ammonite zones (Fig. 8) evidences some discrepancies in the succession of events of the Mattioli & Erba (1999) zonation.

Moreover, the age of a few datums has changed after more than two decades of investigations. In Figure 8 we propose the revision of the Tethyan zonal scheme (Mattioli & Erba 1999) on the basis of reproducibility of single events and their ammonite-calibrated age.

The NJT 5 and NJT 6 Zones remain as proposed by Mattioli & Erba (1999) with the subdivision of the NJT6a and NJT 6b Subzones based on the LO of *M. jansae* as suggested by Ferreira et al. (2019). The base of the NJT 7 Zone is still defined by the FO of *D. striatus* of latest early Toarcian age. Following the proposal of Ferreira et al. (2019) we subdivide three subzones within the NJT 7 Zone using the FOs of *W. colacicchii* (base of NJT 7b Subzone) and *D. criotus* (base of NJT 7c Subzone). According to the ammonite-calibrated ages of these events, the NJT 7b Subzone is early middle Toarcian in age and the NJT 7c Subzone covers the middle middle Toarcian to upper Toarcian interval.

As discussed above, *R. incompta* is extremely rare and sporadic in all Tethyan sections and should not be used as zonal marker. We suggest, instead, to adopt the FO of *W. contracta* to place the base of the NJT 8 Zone in the uppermost Toarcian. Furthermore, since the FOs of *C. magharensis minor* and *W. britannica minor* were proved to be reliable and reproducible, we propose to use these events to fix the base of the NJT 8b and NJT 8c Subzones, respectively. The NJT 9 Zone remains defined by the FO of *W. britannica britannica* of latest Aalenian age as proposed by Mattioli & Erba (1999).

Ferreira et al. (2019) demonstrated that Early-Middle Jurassic calcareous nannofossil events can provide a high-resolution chronostratigraphy through the identification of stage and substage boundaries. Thus, the revised nannofossil zonation allows to place the Toarcian/Aalenian boundary in the NJT 8a Subzone and the Aalenian/Bajocian boundary in the lowermost part of the NJT 9 Zone. Furthermore, the early/middle Toarcian boundary falls within the NJT 7a Subzone and the middle/late Toarcian boundary in the middle part of the NJT 7c Subzone. The early/middle and middle/late Aalenian boundaries correlates with the NJT 8b and NJT 8c Subzones, respectively. In Figure 9 the revised nannofossil zonation and derived chronostratigraphy (Ferreira et al. 2019) is applied to the Colle di Sogno section.

## EVOLUTION OF GENUS *WATZNAUERIA* IN THE TOARCIAN-EARLY BAJOCIAN INTERVAL

The evolution of genus *Watznaueria* was originally reconstructed by Cobianchi et al. (1992) who recognized a general increase in size paralleled by a reduction of the central area in species subsequently appearing in the Toarcian-Bajocian interval. Suchéras-Marx et al. (2012) ascribed the initial diversification of the genus *Watznaueria* (early Bajocian) to the beginning of the coccolithophore lithogenetic contribution in the ocean, coeval with a major C cycle perturbation evidenced by a positive  $\delta^{13}\text{C}$  excursion documented at supraregional scale (Bartolini et al. 1996, 1999; Hesselbo et al. 2003; O'Dogherty et al. 2006; Erba et al. 2019b). Suchéras-Marx et al. (2015) further discussed the emergence of *Watznaueria* in the late Aalenian-early Bajocian interval, emphasizing the biogenic calcite contribution of the genus due to its abundance dominance starting in the early Bajocian.

The works by Suchéras-Marx et al. (2012, 2015) are focused on the biogenic calcite contribution by the genus *Watznaueria*, correlating its emergence - in terms of diversification and increase in abundance - with paleoceanographic/paleoclimatic changes in the early Bajocian. The current study applies the revised taxonomy and chronostratigraphy of *Watznaueria* species, and we comment on the successive morphometric modifications documented in the Toarcian-Aalenian interval, regardless of the implications for the calcareous nannoplankton assemblages and micrite contribution.

The first *Watznaueria* species, namely *W. fos-sacincta* appeared in the early Toarcian. It presents a small open central area and is followed by species possessing a structure in the central area: first *Watznaueria* with a cross (*W. colacicchii* followed by *W. contracta*), then *Watznaueria* with a double-button bridge (*W. gaetanii*), and then *Watznaueria* with a single bridge (*W. britannica minor* and *W. britannica britannica*). As previously underlined by Cobianchi et al. (1992), a progressive increase in size of *Watznaueria* specimens was measured both at generic and species levels (Fig. 10A). An increase of the W/w ratio was detected in successive species indicating the progressive closure of the central area passing from *W. colacicchii* to *W. contracta*, *W. gaetanii*, *W. britannica minor* and *W. britannica britannica* (Fig. 10B). Moreover, the structure in the central area shows

a modification from a cross (*W. colacicchii* and *W. contracta*) to a double-button bridge (*W. gaetanii*) to a single-button bridge (*W. britannica minor* and *W. britannica britannica*) (Fig. 9). In the late Aalenian *W. communis* appeared; its thick bridge in the central area, optically continuous with the inner cycle of the coccolith, could be the transition to younger *Watznaueria* species with a closed central area such as *W. manivittiae* and *W. barnesiae* which first occur in the lower Bajocian and lowermost Bathonian, respectively.

The morphometric variations here documented in *Watznaueria* coccoliths took place starting from the middle Toarcian through the late Aalenian, with definitively faster evolutionary rates in the Aalenian, apparently during a stable and oligotrophic regime (e.g. Aguado et al. 2008). This is not surprising since other evolutionary innovations, especially intragenerically, in the Mesozoic history of calcareous nannoplankton correlate with times of paleoceanographic stability and low trophic levels (e.g. Erba 2006).

## CONCLUSIONS

High-resolution calcareous nannofossil biostratigraphy of the Colle di Sogno section allowed the identification of 24 events in the Toarcian-lower Bajocian interval. The general frequent to common abundance and poor to moderate preservation of nannofossil assemblages resulted in the recognition of the NJT5 to NJT9 Zones, further subdivided in subzones. The biozonation of Mattioli & Erba (1999) was revised taking into account new/additional nannofossil biohorizons and reassessed ages of a few events.

Morphometric investigations of the genus *Watznaueria* allowed to differentiate *W. colacicchii* from *W. contracta* (W/w ratio), and *W. britannica britannica* from *W. britannica minor* (coccolith L). The new species *W. gaetanii* was described. In the Toarcian-Aalenian interval a progressive increase in size of *Watznaueria* specimens was documented - both at generic and species levels - paralleled by the progressive closure of the central area (increase of the W/w ratio) passing from *W. colacicchii* to *W. contracta*, *W. gaetanii* and the *W. britannica* group. Moreover, the structure in the central area shows a modification from a cross (*W. colacicchii* and *W. contracta*) to a

double-button bridge (*W. gaetanii*) to a single-button bridge (*W. britannica minor* and *W. britannica britannica*). Such interspecific evolutionary innovations accelerated in the Aalenian characterized by a paleoceanographic stable and oligotrophic regime.

*Acknowledgments:* We gratefully acknowledge the constructive criticisms by the Associate Editor Silvia Gardin, the Reviewer Fabienne Giraud and two anonymous Reviewers. The research was funded by MIUR- PRIN 2017RX9XXXV awarded to EE.

#### REFERENCES

- Aguado R., O'Dogherty L. & Sandoval J. (2008) - Fertility changes in surface waters during the Aalenian (mid-Jurassic) of the Western Tethys as revealed by calcareous nannofossils and carbon-cycle perturbations. *Marine Micropaleontology*, 68(3-4): 268-285.
- Baghli H., Mattioli E., Spangenberg J.E., Ruebsam W., Schwark L., Bensalah M., Sebane A., Pittet B., Pellenard P. & Suan G. (2022) - Stratification and productivity in the Western Tethys (NW Algeria) during early Toarcian. *Palaeogeography, Palaeoclimatology, Palaeoecology*, 591: 110864.
- Bartolini A., Baumgartner P.O. & Hunziker J.C. (1996) - Middle and Late Jurassic carbon stable-isotope stratigraphy and radiolarite sedimentation of the Umbria-Marche Basin (Central Italy). *Eclogae Geologicae Helveticae*, 89: 811-844.
- Bartolini A., Baumgartner P.O. & Guex J. (1999) - Middle and Late Jurassic radiolarian palaeoecology versus carbon-isotope stratigraphy. *Palaeogeography, Palaeoclimatology, Palaeoecology*, 145(1-3): 43-60.
- Bernoulli D. & Jenkyns H.C. (1974) - Alpine Mediterranean and central Atlantic Mesozoic facies in relation to the early evolution of the Tethys. In Dott R.H. & Shaver R.H. (Eds) - Modern and ancient geosynclinal sedimentation: *Society and Economic Paleontologists and Mineralogists Special Publication*, 18: 129-160.
- Bernoulli D. & Jenkyns H.C. (2009) - Ancient oceans and continental margins of the Alpine-Mediterranean Tethys: Deciphering clues from Mesozoic pelagic sediments and ophiolites. *Sedimentology*, 56(1): 149-190.
- Bosence D., Procter E., Aurell M., Bel Kahla A., Boudagher-Fadel M., Casaglia F., Cirilli S., Mehdie M., Nieto L., Rey J., Scherreiks R., Soussi M. & Waltham D. (2009) - A dominant tectonic signal in high-frequency, peritidal carbonate cycles? A regional analysis of Liassic platforms from western Tethys. *Journal of Sedimentary Research*, 79(6): 389-415.
- Bown P.R. (1987) - Taxonomy, evolution, and biostratigraphy of Late Triassic-Early Jurassic calcareous nannofossils. *Palaeontological Association, Special papers on Palaeontology*, 32: 1-118.
- Bown P.R. & Cooper M.K.E. (1989) - New calcareous nannofossil taxa from the Jurassic. *Journal of Micropaleontology*, 8(1): 91-96.
- Bown P.R. & Cooper M.K.E. (1998) - Jurassic. In: Bown P.R. (Ed.) - Calcareous nannofossil biostratigraphy. *British Micropaleontological Society Published Series*: 34-85. Kluwer Academic Publishers, London.
- Bown P.R., Lees J.A. & Young J.R. (2004) - Calcareous nannoplankton evolution and diversity through time. In: Thierstein H.R. & Young J.R. (Eds) - Coccolithophores: from molecular processes to global impact: 481-508. Springer, Berlin, Heidelberg.
- Casellato C.E. & Erba E. (2015) - Calcareous nannofossil biostratigraphy and paleoceanography of the Toarcian Oceanic Anoxic event at Colle di Sogno (southern Alps, northern Italy). *Rivista Italiana di Paleontologia e Stratigrafia*, 121(3): 297-327.
- Channell J.E.T., Casellato C.E., Muttoni G. & Erba E. (2010) - Magnetostratigraphy, nannofossil stratigraphy and apparent polar wander for Adria-Africa in the Jurassic - Cretaceous boundary interval. *Palaeogeography, Palaeoclimatology, Palaeoecology*, 293(1-2): 51-75.
- Cobianchi M., Erba E. & Pirini Radrizzani C. (1992) - Evolutionary trends of calcareous nannofossil genera *Lotharingius* and *Watznaueria* during the Early and Middle Jurassic. *Memorie di Scienze Geologiche*, 43: 19-25.
- Cresta S., Goy A., Ureta S., Arias C., Barroon E., Bernard J., Canales M.L., García-Joral F., García-Romero E., Gialanella P.R., Gómez J.J., González J.A., Herrero C., Martínez G., Osete M.L., Perilli N. & Villalaín J.J. (2001) - The Global Boundary Stratotype Section and Point (GSSP) of the Toarcian-Aalenian Boundary (Lower-Middle Jurassic). *Episodes*, 24(3): 166-175.
- Erba E. (1990) - Calcareous nannofossil biostratigraphy of some Bajocian sections from the Digne area (SE France). *Memorie descrittive della Carta Geologica d'Italia*, 60: 237-256.
- Erba E. (2006) - The first 150 million years history of calcareous nannoplankton: Biosphere - Geosphere interaction. *Palaeogeography, Palaeoclimatology, Palaeoecology*, 232: 237-250.
- Erba E., Gambacorta G., Visentin S., Cavalheiro L., Reolon D., Faucher G. & Pegoraro M. (2019a) - Coring the sedimentary expression of the Early Toarcian Oceanic Anoxic Event: new stratigraphic records from the Tethys Ocean. *Scientific Drilling*, 7: 1-12.
- Erba E., Gambacorta G. & Tiepolo M. (2019b) - The Gaetani Level: a potential oceanic anoxic event of early Bajocian age (Middle Jurassic). *Rivista Italiana di Paleontologia e Stratigrafia*, 124: 219-230.
- Erba E., Cavalheiro L., Dickson A.J., Faucher G., Gambacorta G., Jenkyns H.C. & Wagner T. (2022) - Carbon and oxygen-isotope signature of the Toarcian Oceanic Anoxic Event: insights from two Tethyan pelagic sequences (Gajum and Sogno Cores-Lombardy Basin, northern Italy). *Newsletters on Stratigraphy*, 55: 451-477.
- Fantasia A., Mattioli E., Spangenberg J.E., Adatte T., Bernárdez E., Ferreira J., Thibault N., Krencker F.-N. & Bodin S. (2022) - The middle-late Aalenian event: A precursor of the Mesozoic Marine Revolution. *Global and Planetary Change*, 208: 103705.

- Ferreira J., Mattioli E., Sucheràs-Marx B., Giraud F., Duarte V. L., Pittet B., Suan G., Hassler A. & Spangenberg J.E. (2019) - Western Tethys Early and Middle Jurassic calcareous nannofossil biostratigraphy. *Earth-Science Reviews*, 197: 1-19.
- Fraguas A., Comas-Rengifo M.J. & Perilli N. (2015) - Calcareous nannofossil biostratigraphy of the Lower Jurassic in the Cantabrian Range (Northern Spain). *Newsletter on Stratigraphy*, 48(2): 179-199.
- Fraguas Á., Comas-Rengifo M.J., Goy A. & Gómez, J.J. (2018) - Upper Sinemurian-Pliensbachian calcareous nannofossil biostratigraphy of the E Rodiles section (Asturias, N Spain): a reference section for the connection between the Boreal and Tethyan Realms. *Newsletters on Stratigraphy*, 51(2): 227-244.
- Gaetani M. (1975) - Jurassic stratigraphy of the Southern Alps: a review. *Geology of Italy*, 1: 377-402.
- Gaetani M. (2010) - From Permian to Cretaceous: Adria as pivotal between extensions and rotations of Tethys and Atlantic Oceans. In: Beltrando M., Peccerillo A., Mattei M., Conticelli S. & Doglioni C. (Eds) - *Geology of Italy. Journal of the Virtual Explorer*, 36: 5.a.
- Gaetani M. & Poliani G. (1978) - Il Toarciano e il Giurassico medio in Albenza (Bergamo). *Rivista Italiana di Paleontologia e Stratigrafia*, 84: 349-382.
- Gaetani M. & Erba E. (1990) - Il Bacino Lombardo: un sistema paleoalto/fossa in un margine continentale passivo durante il Giurassico. 75° Congresso Società Geologica Italiana. Guida alle escursioni precongresso. Escursione A3.
- Giraud F. (2009) - Calcareous nannofossil productivity and carbonate production across the Middle-Late Jurassic transition in the French Subalpine Basin. *Geobios*, 42(6): 699-714.
- Giraud F., Pittet B., Mattioli E. & Audouin V. (2006) - Paleoenvironmental controls on the morphology and abundance of the coccolith *Watznaueria britannica* (Late Jurassic, southern Germany). *Marine Micropaleontology*, 60(3): 205-225.
- Hesselbo S.P., Morgans-Bell H.S., McElwain J.C., Rees P.M., Robinson S.A. & Ross C.E. (2003) - Carbon-cycle perturbation in the Middle Jurassic and accompanying changes in the terrestrial paleoenvironment. *The Journal of Geology*, 111(3): 259-276.
- Hinnov L.A., Park J. & Erba E. (2000) - Lower-Middle Jurassic rhythmites from the Lombard Basin, Italy: a record of orbitally forced carbonate cycles modulated by secular environmental changes in West Tethys. In: Hall R. L. & Smith P. L. (Eds) - *Advances in Jurassic Research 2000. GeoResearch Forum*, 6: 427-436. Trans Tech Publications Zurich, Switzerland.
- Jenkyns H.C. & Clayton C.J. (1986) - Black shales and carbon isotopes in pelagic sediments from the Tethyan Lower Jurassic. *Sedimentology*, 33: 87-106.
- Jenkyns H.C. (2020) - The demise and drowning of Early Jurassic (Sinemurian) carbonate platforms: stratigraphic evidence from the Italian peninsula, Sicily and Spain. In: L'Eredità scientifica di Paolo Scandone, *Atti dei Convegni Lincei* 335: 55-82.
- Mattioli E. (1996) - New calcareous nannofossil species from the Early Jurassic of Tethys. *Rivista Italiana di Paleontologia e Stratigrafia*, 102: 397-412.
- Mattioli E. & Erba E. (1999) - Synthesis of calcareous nannofossil events in Tethyan Lower and Middle Jurassic successions. *Rivista Italiana di Paleontologia e Stratigrafia*, 105: 343-376.
- Menini A., Mattioli E., Spangenberg J.E., Pittet B., Suan G. (2019) - New calcareous nannofossil and carbon isotope data for the Pliensbachian/Toarcian boundary (Early Jurassic) in the western Tethys and their paleoenvironmental implications. *Newsletters on Stratigraphy*, 52, 2: 173-196.
- Molina J.M., Reolid M. & Mattioli E. (2018) - Thin-shelled bivalve buildup of the lower Bajocian, South Iberian paleomargin: development of opportunists after oceanic perturbations. *Facies*, 64: 1-17.
- Monechi S. & Thierstein H.R. (1985) - Late Cretaceous-Eocene nannofossil and magnetostratigraphic correlations near Gubbio, Italy. *Marine Micropaleontology*, 9: 419-440.
- Muttoni G., Erba E., Kent D.V. & Bachtadse V. (2005) - Mesozoic Alpine facies deposition as a result of past latitudinal plate motion. *Nature*, 434, 7029: 59-63.
- O'Dogherty L., Sandoval J., Bartolini A., Bruchez S., Bill M. & Guex J. (2006) - Carbon-isotope stratigraphy and ammonite faunal turnover for the Middle Jurassic in the Southern Iberian paleomargin. *Palaeogeography, Palaeoclimatology, Palaeoecology*, 239: 311-333.
- Olivier N., Pittet B. & Mattioli E. (2004) - Paleoenvironmental control on sponge-microbialite reefs and contemporaneous deep-shelf marl-limestone deposition (Late Oxfordian, southern Germany). *Palaeogeography, Palaeoclimatology, Palaeoecology*, 212: 233-263.
- Pasquini C. & Vercesi P.L. (2002) - Tettonica sinsedimentaria e ricostruzione paleogeografica del margine occidentale dell'Alto dei Corni Di Canzo nel Lias inferiore. *Memorie della Società Geologica Italiana*, 57: 107-114.
- Pittet B. & Mattioli E. (2002) - The carbonate signal and calcareous nannofossil distribution in an Upper Jurassic section (Balingen-Tieringen, Late Oxfordian, southern Germany). *Palaeogeography, Palaeoclimatology, Palaeoecology*, 179: 71-96.
- Reinhardt P. (1964) - Einige Kalkflagellaten-Gattungen (Coccolithophoriden, Coccolithineen) aus dem Mesozoikum Deutschlands. *Monatsberichte der Deutschen Akademie der Wissenschaften zu Berlin*, 6: 749-759.
- Roth P.H. (1983) - Jurassic and Lower Cretaceous calcareous nannofossil in the Western North Atlantic (Site 534): biostratigraphy, preservation, and some observations on biogeography and paleoceanography. *Initial Reports Deep Sea Drilling Project*, 76: 587-621.
- Roth P.H. & Thierstein H.R. (1972) - Calcareous nannoplankton: Leg 14 of the DSDP. In: Hayes D.E., Primm A.C., et al. (Eds.) - *Initial reports of the Deep Sea Drilling Project*, 14: 421-485.
- Sandoval J., O'Dogherty L., Aguado R., Bartolini A., Bruchez S. & Bill M. (2008) - Aalenian carbon-isotope stratigraphy: calibration with ammonite, radiolarian and nan-

- nofossil events in the Western Tethys. *Palaeogeography, Palaeoclimatology, Palaeoecology* 267: 115-137.
- Sandoval J., Bill M., Aguado R., O'Dogherty L., Rivas P., Morard A. & Guex J. (2012) - The Toarcian in the Subbetic basin (southern Spain): Bio-events (ammonite and calcareous nannofossils) and carbon-isotope stratigraphy. *Palaeogeography, Palaeoclimatology, Palaeoecology*, 342: 40-63.
- Santantonio M. & Carminati E. (2011) - The Jurassic rifting evolution of the Apennines and Southern Alps (Italy): Parallels and differences. *Bulletin of the Geological Society of America*, 124: 468-484.
- Scotese C.R. (2011) - The PALEOMAP Project PaleoAtlas for ArcGIS, Volume 3, Jurassic and Triassic Paleogeographic and Plate Tectonic Reconstructions, version (9.2r). PALEOMAP Project, Arlington, Texas.
- Stradner H. (1963) - New contributions to Mesozoic stratigraphy by means of nannofossils. *Proceedings of the Sixth World Petroleum Congress*, Section I, Paper 4: 167-183.
- Suchéras-Marx B., Guihou A., Giraud F., Lécuyer C., Allemand P., Pittet B. & Mattioli E. (2012) - Impact of the Middle Jurassic diversification of *Watznaueria* (coccolith-bearing algae) on the carbon cycle and  $\delta^{13}\text{C}$  of bulk marine carbonates. *Global and Planetary Change*, 86: 92-100.
- Suchéras-Marx B., Mattioli E., Giraud F. & Escarguel G. (2015) - Paleoenvironmental and paleobiological origins of coccolithophorid genus *Watznaueria* emergence during the late Aalenian-early Bajocian. *Paleobiology* 41: 415-435.
- Tiraboschi D. & Erba E. (2010) - Calcareous nannofossil biostratigraphy (Upper Bajocian-Lower Bathonian) of the Ravin du Bès section (Bas Auran, Subalpine Basin, SE France): evolutionary trends of *Watznaueria barnesiae* and new findings of “*Rucinolithus*” morphotypes. *Geobios*, 43: 59-76.
- Tremolada F., Erba E., van de Schootbrugge B. & Mattioli E. (2006) - Calcareous nannofossil changes during the late Callovian-early Oxfordian cooling phase. *Marine Micropaleontology*, 59: 197-209.
- Visentin S. & Erba E. (2021) - High-resolution calcareous nannofossil biostratigraphy across the Toarcian Oceanic Anoxic Event in northern Italy: clues from the Sogno and Gajum Cores (Lombardy Basin, Southern Alps). *Rivista Italiana di Paleontologia e Stratigrafia*, 127: 539-556.
- Visentin S., Faucher G., Mattioli E. & Erba E. (2021a) - Taxonomic revision of the genus *Carinolithus* (Early-Middle Jurassic) based on morphometric analyses and diagenesis observations: Implications for biostratigraphy and evolutionary trends. *Marine Micropaleontology*, 162: 101950.
- Visentin S., Erba E. & Mutterlose J. (2021b) - Bio - and chemostratigraphy of the Posidonia Shale: a new database for the Toarcian Oceanic Anoxic Event from northern Germany. *Newsletters on Stratigraphy*, DOI:10.1127/nos/2021/0658.
- Winterer E.L. & Bosellini A. (1981). Subsidence and sedimentation on Jurassic passive continental margin, Southern Alps, Italy. *AAPG Bulletin*, 65(3): 394-421.